Final Thesis

Operation of a high-power fuel cell for automotive traction

Student: João Victor Cruz Antonio Saraiva
Tutor: Marcelo Seckler

19th April 2024

SUMMARY

Hydrogen for automotive transportation is becoming a reality, both for economic activities and leisure purposes. For over two years, the hosting group has been working on a concept of hydrogen-powered electric vehicle suitable for urban and peri-urban transport. The objective is to combine the fuel cell of a Kangoo ZE Hydrogen with supercapacitors to ensure vehicle dynamics and save energy required for the journey. The aim of this Master's research project is to study the fuel cell system of the considered vehicle, which consists of the fuel cell itself, with its electrochemical cells providing a power of 5 kW, the gas distribution system (air, hydrogen), the cooling water system for the fuel cell, and the heat exchanger. The goal is to correlate the voltage and power of the fuel cell with the current, as well as the gas and heat flow evacuated by the system. The work on this fuel cell will be conducted on the new hydrogen platform at the Faculty of Science and Technology in Nancy. The tests on the 5 kW fuel cell will be carried out investigating different parameters related to performance and needs of the system, following an introductory phase at the laboratory scale (150 W) at the ENSIC site. To enhance comprehension of fuel cell technology and electrochemistry concepts within the domain, a thorough bibliographic research will be conducted prior to commencing the fuel cell experiments. This research aims to delve into a wide range of relevant literature, thereby facilitating a comprehensive understanding of the subject matter ensuring informed experimentation and analysis in the subsequent stages.

1. Introduction

There is a growing concern about the impact of climate change as the situation becomes increasingly pessimistic year by year. For almost three decades, the United Nations (UN) has brought together nearly every country on earth for global climate summits, known as COPs, to discuss and promote multilateral action on climate change. The COPs were born at the Earth Summit in Rio in 1992, when over 178 countries met for the ten-year UN conference on environment and development and signed the Rio de Janeiro Declaration on Environment and Development, which defined sustainable development.[(1)]

The 26th edition of the COP was recently held in Glasgow, with a focus on implementing the Paris Agreement through actions to promote a more sustainable, low-carbon future. One of the most significant decisions made at the summit was the agreement to phase-down coal power and phase-out "inefficient" fossil fuel subsidies, two key issues that had never been explicitly mentioned in UN climate talks before[(2)]. This decision was critical in the fight against global warming, as coal, oil, and gas are the primary drivers of climate change.

Transportation is responsible for approximately 25% of global greenhouse gas emissions, with road transport alone accounting for around 10%. As a result, it is crucial to explore alternative solutions with lower emissions that are suitable for large-scale use. While many automobile giants have already shifted towards battery-powered vehicles, these come with significant drawbacks such as long charging times, relatively high costs, and short lifespans.

The proton exchange membrane fuel cell (PEMFC) is a relatively new technology that is receiving increasing attention in the automobile industry as a promising alternative to both fossil fuel-driven vehicles and battery vehicles. The technology, also known as polymer electrolyte membrane fuel cells, requires hydrogen as fuel and has shown promising results in terms of performance and advantages.

In addition to its potential as an alternative to fossil fuel-powered and battery-powered vehicles, PEMFC technology also has other potential applications in the field of energy production. For example, PEMFCs can be used in portable electronic devices, as they are lightweight and have a high energy density. They can also be used in stationary power

systems, such as backup generators for buildings, where their high efficiency and low emissions make them a desirable option. As research and development in the field of PEMFCs continues, it is likely that their applications will expand even further, making them an increasingly important technology in the effort to mitigate the effects of climate change and transition towards a more sustainable future.

This report will provide an overview of the PEMFCs and analyze various aspects around the hydrogen-driven technology to assess its performance. The studies will be conducted at two levels, the first being on an experimental bench located at LRGP (Laboratoire Réactions et Génie des Procédés) for a 100 cm^2 five-cell stack. The second level will consist of tests at a platform located in the Faculté des Sciences de Nancy, being administered at a 5,0 kW fuel cell aiming to charge the battery of a Kangoo ZE, thus presenting an alternative for the more traditional methods. Additionally, the study will investigate and discuss air circulation, humidity of the membrane and other important aspects to ensure fast fueling and affordability.

2. General aspects of fuel cells

Fuel cells are devices able to convert chemical energy into electrical energy, they work by using an electrochemical process to convert hydrogen and oxygen into water, while producing electricity in the process. Fuel cells can present a number of advantages over conventional combustion engines, including higher efficiency, reduced emissions, and lower noise levels and they present themselves in different types such as alkaline fuel cell, phosphoric acid fuel cell or solid acid fuel cell, among others. Those types vary between them in species of fuel and electrolyte, working temperature and efficiency, besides application and level of maturation. Some of the examples of fuel cells are listed below.

Fuel cell	Temperature (°C)	Efficiency (%)	Electrolyte
AFC	50-90	50-70	Aqueous solution of potassium hydroxide soaked matrix
PAFC	175-220	40-45	Phosphoric acid soaked in a matrix
MCFC	600-650	50-60	Solution of lithium, sodium and/or potassium carbonates soaked in a matrix
SOFC	800-1000	50-60	Solid zirconium oxide with a small amount of yttrium as Y_2O_3
PEMFC*	60-100	40-50	Solid organic polymer
DMFC*	50-120	25-40	Solid organic polymer

Table 1: main features of different types of fuel cells

The asterisks are placed to indicate that the direct methanol fuel cell (DMFC) is actually a subcategory of PEMFCs that uses methanol as the fuel, whereas the conventional fuel for PEMFCs is often hydrogen, as it will be discussed further. [9]

2.1 Proton Exchange Membrane Fuel Cell (PEMFCs)

In this section, the fundamentals of fuel cells categorized as PEMFC, one of the leading technologies in the perspective of creating a decarbonized yet efficient automobile industry, will be presented.

- Principle

Just like any other fuel cell, PEMFC's main goal is to produce electrical energy. It operates with hydrogen as a fuel and oxygen as the oxidant agent, the latter being usually in the form of air. The main reactions found are therefore:

Anode: $2H_2 \longrightarrow 4H^+ + 4e^-$ (1)

Cathode: $O_2 + 4e^- + 4H^+ \longrightarrow 2H_2O$ (2)

As it is possible to observe, protons that shall permeate through the membrane in direction to the cathode are produced at the anode electrode (Figure 1). Once at the cathode electrode, these protons will be consumed in order to reduce the oxygen coming from the air thus producing water. The overall equation is represented by:

Global reaction: $2H_2 + O_2 \longrightarrow 2H_2O$ (3)

This reaction is exothermic and releases around Δh_f = -241,83kJ per mol of steam water produced at the temperature of 25ºC under atmospheric pressure. If this steam is condensed afterwards, the energy release goes up to Δh_f = -285,84kJ at the same conditions. Those two enthalpies are named respectively lower heating value (LHV) and higher heating value (HHV). As it will be discussed later, a part of this energy will turn into electrical power while the rest will be dissipated as heat. [7]

- Elements

The PEMFC is divided into two major parts, the flow plates (FP) and the actual membrane assembly (MEA). The latter contains the proton exchange membrane itself (PEM), the catalyst layer (CL) which acts as the electrode and the gas diffusion layer. The role of each of these elements will be further explained.

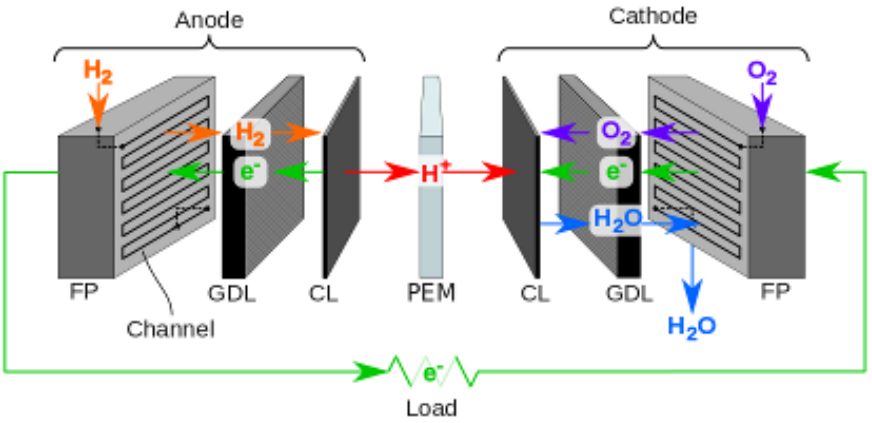

Figure 1: Different elements of a fuel cell and electrode reactions

Flow plates: also known as bipolar plates, the flow plates contain gas channels on one side for even distribution of the reacting gases and water channels on the other side in order to control the temperature of the fuel cell. It also presents a series of purposes besides temperature control: being the exoskeleton structure of the PEMFC, it conducts electrons from the electrode surface to the terminal plate, besides promoting the control of the temperature by allowing a heat flux and supply or removal of fluids such as gas and liquid water if any.

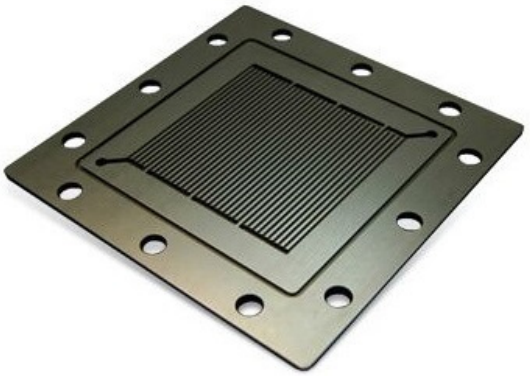

Figure 2: example of a flowplate's design

Proton exchange membrane: the PEM, as the name suggests, is a polymer-based membrane that allows the passage of protons whereas not allowing the passage of electrons, gases or eventually other ions. This phenomenon is possible due to the presence of sulfonate groups crafted at the membrane added to the existence of an electrical field. The protons are always hydrated, their passage through the membrane is accompanied by water transfer to the anode. The membrane separates the two electrodes and forces the passage of electrons to occur from the anode to the cathode through an external circuit.

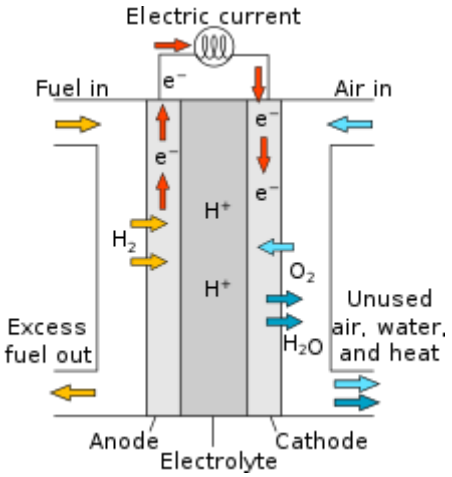

Figure 3: membrane scheme

Catalyst layer: platinum is the most common catalyst employed as it is very effective for hydrogen oxidation and hydrogen reduction. The platinum material is usually supported by activated carbon as it presents greater internal surface area and lower cost per cubic meter compared to other carriers such as silica or alumina.[7] The catalyst layer forms the cathode and the anode, and their design is of a great importance to allow the occurrence of the reactions at a desirable rate.

Gas diffusion layer: this component is placed between the bipolar plate and the catalyst layer. The GDL allows better diffusion and transport of gases besides preventing the flooding of the fuel cell due to the water production, which damages the efficiency of the FC and the physical structure of the catalyst. Being the outermost part of the membrane assembly, the GDL also protects the catalyst layers which are perceived to be much more fragile. [7]

3. State of art and bibliography

Proton exchange membrane fuel cells (PEMFCs) have gained significant attention as a promising technology for sustainable urban mobility. With zero emissions and high efficiency, PEMFCs can offer an attractive alternative to conventional internal combustion engines. In this report, we will discuss the state of the art in PEMFC technology applied to urban mobility. One of the main challenges facing the adoption of PEMFCs in urban mobility is the limited availability of hydrogen refueling infrastructure. However, recent efforts to expand the network of hydrogen refueling stations have improved the accessibility of hydrogen fuel for vehicles equipped with PEMFCs. As of 2023, there are over 250 hydrogen refueling stations in Europe, with plans to increase this number significantly in the coming years.[12]

Another important aspect of PEMFC technology for urban mobility is the development of high-performance fuel cell systems that are compact and lightweight. Recent advancements in materials science and system design have led to the development of more efficient and durable fuel cell stacks that can be integrated into compact and lightweight systems suitable for urban mobility. Furthermore, research is ongoing to improve the durability of PEMFCs, particularly in the harsh operating conditions of urban mobility. Researchers are exploring the

use of advanced materials, coatings, and designs to enhance the stability and durability of PEMFCs, as well as developing new diagnostic and prognostic tools for monitoring the health of the fuel cell system.

Moreover, advances in control and power management systems are improving the performance and reliability of PEMFCs in urban mobility. Sophisticated control algorithms are being developed to optimize the operation of fuel cell systems in response to changing driving conditions and demands, as well as to maximize energy recovery during regenerative braking. Additionally, the integration of PEMFCs with battery systems is a key area of research in the field of urban mobility. By combining the advantages of both technologies, such as the high power density of PEMFCs and the energy storage capacity of batteries, it is possible to create hybrid systems that offer improved performance, range, and efficiency.[11]

The state of the art in PEMFC technology applied to urban mobility is therefore focused on improving the availability and accessibility of hydrogen refueling infrastructure, developing high-performance and durable fuel cell systems, improving control and power management systems, and exploring the integration with battery systems. As research in this field continues to advance, PEMFCs have the potential to play a significant role in creating sustainable and efficient urban mobility solutions.

4. Installations, materials and methods

During the initial weeks of the project, studies have been conducted on both an 150 W laboratory-scaled experimental bench as well as at a platform containing a 5,0 kW fuel cell prompted to recharge an electrical car, the Kangoo ZE. The faculties of each of these systems will be detailed further, and their characteristics will be explored in this section.

4.1 Experimental bench

The experimental bench utilized in this study consisted of a 100 cm^2 UBzM PEMFC containing a stack of 5 cells, located at the capacities of the ‘Laboratoire des Réactions et Génie des Procédés’ (LRGP) in Nancy. The system also included mass flow rate controllers, gas mixing chamber, humidifier, temperature controller among other essential elements.

Figure 4 exhibited below provides a visual representation of the system while Figure 5 provides a visualization of the process.

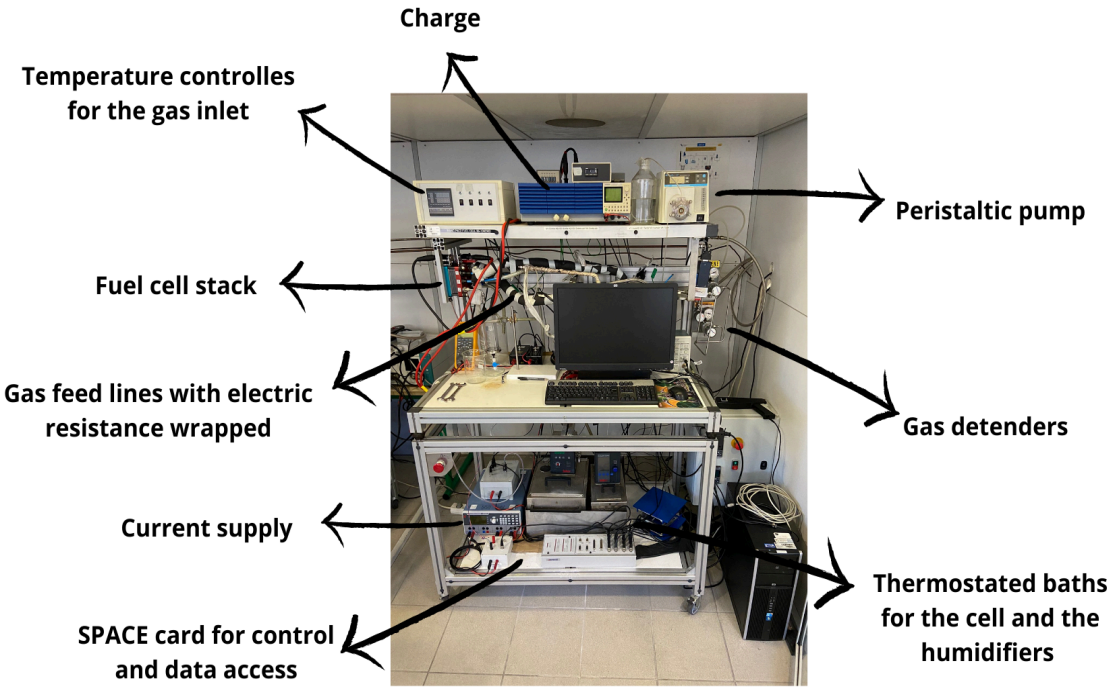

Figure 4: experimental bench located at ENSIC

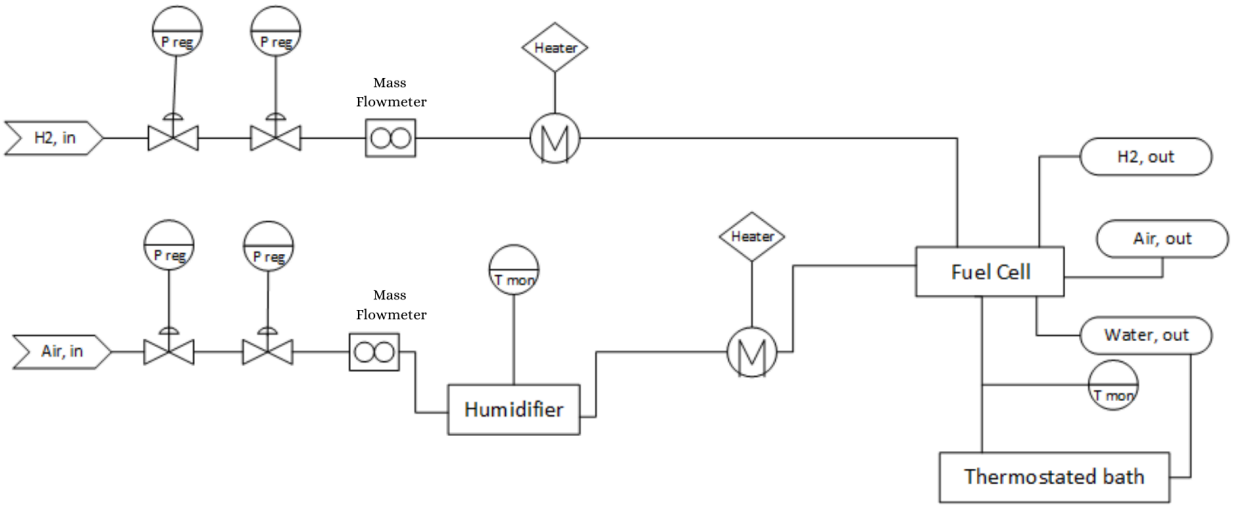

Figure 5: process flow diagram of the test bench

The software SPACE was used to initiate, control and monitor the system, tracing the progression of variables such as current, individual voltage and stack voltage. As the results were being recorded, it was possible to perform analysis over variables such as gas flowrate,

tension and power using the notions of electrochemistry and chemical engineering that will be detailed further.

Regarding the steps to operate the system, it must be first ensured that the hydrogen supply and the air supply are connected and the valve is open. It is also fundamental to check that the humidifier contains a desired level of deionised water for the system to operate properly. Once this is confirmed, it is important to verify that the load, the thermostatic bath, the current supply as well as all the other devices indicated in Figure 5 are powered up and working accordingly. After the system has reached the desired temperature, it is possible to initiate it. This is done through SPACE, in which the intensity of current and the stoichiometry factor for hydrogen and oxygen will be set, therefore controlling the fluxes entering the fuel cell.

The system is now operating and it is possible to monitor its results through SPACE, which allows us to trace the evolution of a series of parameters. It is nonetheless essential to acknowledge any abnormalities or malfunctions to ensure that it operates safely and effectively. The test bench was very useful considering the purpose of understanding and analyzing the functioning of a PEMFC, but it didn't have the required magnitude to be connected with an electrical car so further investigation on a larger scale was necessary, which will be described in the next section.

4.2 Platform

The platform is an innovative setting designed to study the feasibility of using fuel cells to power an electric car. The system was equipped with a 5,0 kW fuel cell comprising a 200 cm^2 stack of 70 cells from *Symbio*. Although the principle of the system is similar to the experimental bench described previously, the platform is designed to operate on a larger scale, with different dimensions and components, in order to charge a Kangoo ZE and to optimize the vehicle's dynamics and save energy during a journey.

The supply of hydrogen for the system is provided by two cylinders dedicated to the project, which are located in the laboratory's surroundings. Oxygen is supplied through ambient air from the compressor, with measures in place to ensure temperature and humidity control.

Overall, the platform represents an exciting step forward in the exploration of alternative energy sources for vehicles and has the potential to make a significant impact on reducing carbon emissions. A detailed description of the system is provided in the photos (Figure 6 and Figure 7) and the flowsheet (Figure 8) below.

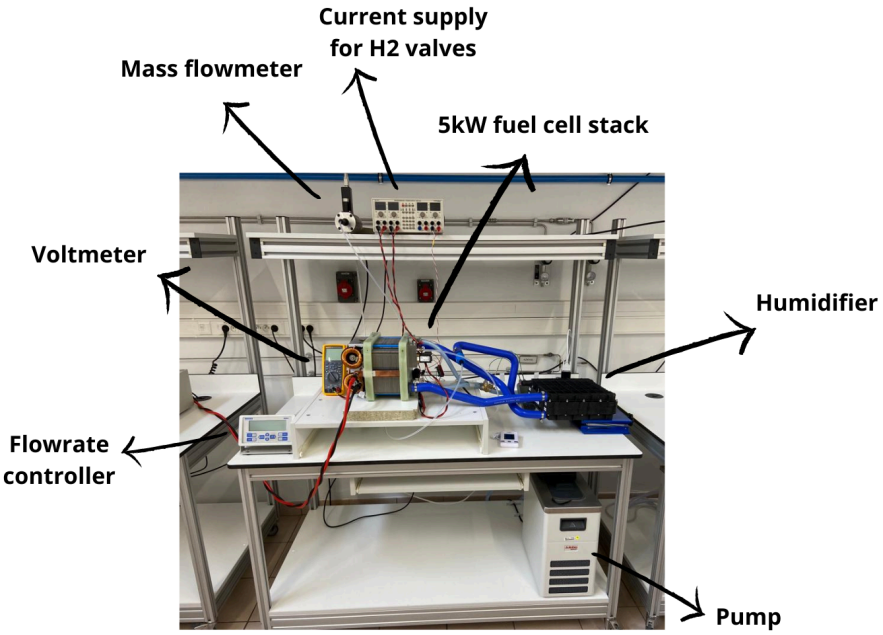

Figure 6: fuel cell system located at the platform

The humidifier shown in the photo is designed to humidify the air stream before it enters the fuel cell, a step that is crucial for the proper functioning of the PEMFC as the membrane requires adequate humidification. The device pictured as the pump is actually a thermostatic bath that serves in the system's configuration as a pump. The purpose of the current supply depicted in the top of the picture is to facilitate the flow of electrons between the anode and the cathode, which is essential for generating an electric current by completing the circuit and allowing the electrons to flow from the anode to the cathode.

Load

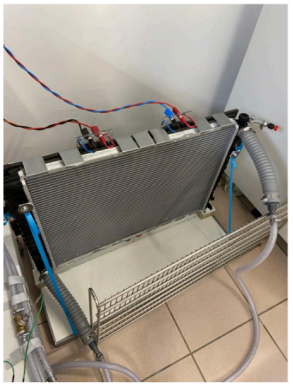

Radiator (for temperature control)

Hydrogen cylinders

Heat exchanger

Vehicle (Kangoo ZE)

Figure 7: other elements of the platform

The load of 2,6 kW is employed to absorb the power produced by the fuel cell while the hydrogen cylinders, situated outside of the facility, are responsible for the hydrogen supply. The heat exchanger, used for the evacuation of the heat produced in the fuel cell, is a *BP400* model from the BPX series, bought from *RS Components*. The radiator also serves for the purpose of temperature control by expelling the heat to the atmosphere using fans, it was removed from a car engine and bought at a local store. The control of fan usage and intensity in the radiator is possible through an external device connected to it, and it is based on the specific requirements for heat dissipation at each test.

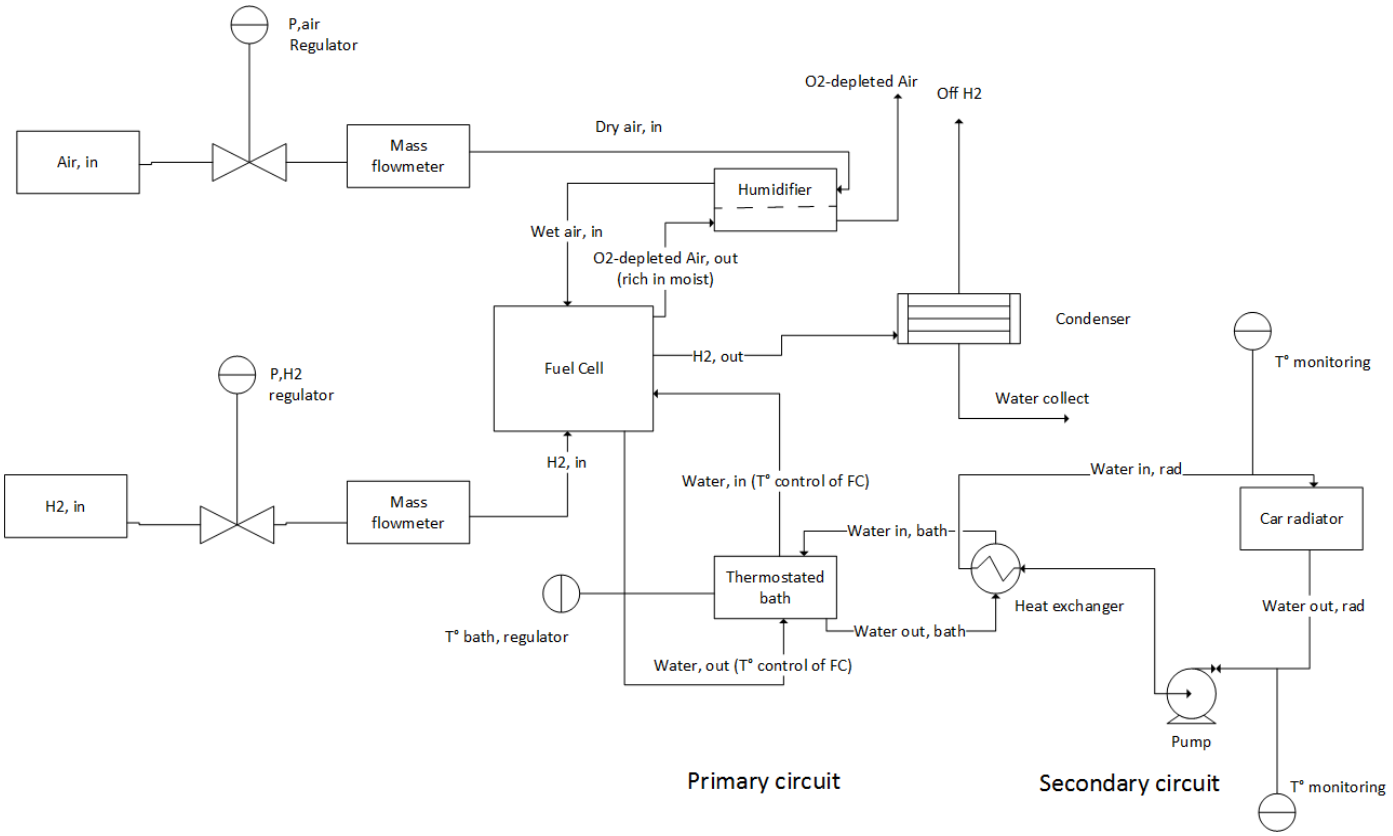

Figure 8: Process flow diagram of the platform system

4.3 Methods and resources

In order to work with proton exchange membrane fuel cells in the context of urban and peri-urban mobility, it is essential to have a solid understanding of several methods and algebraic resources. PEM fuel cells are electrochemical devices that convert the chemical energy of hydrogen and oxygen into electrical energy, therefore understanding the basic principles of electrochemistry, such as redox reactions and electron transfer is essential for working with PEM fuel cells. It is equally important to have notions of thermodynamics, considering that our systems operate under specific thermodynamic conditions, and understanding these conditions is critical for designing and optimizing the performance of the fuel cell system. Concepts such as enthalpy, entropy, Gibbs free energy, and thermodynamic efficiency are important for predicting the behavior of the fuel cell under different operating conditions.

Other resources used for the development of this project are in the field of transport phenomena, as the adequate functioning of the system involves complex transport phenomena, such as mass transport of reactants and products, heat transfer, and charge transport. Understanding the mechanisms of these phenomena and their interactions is crucial for modeling the fuel cell system and optimizing its performance. Lastly, the behavior of PEM fuel cells is often described by algebraic models and mathematical tools, they can be used to predict the performance of the fuel cell under different operating conditions and to optimize the system's design and operation. Key algebraic resources include equations for mass and charge transport, reaction kinetics, and thermodynamic properties.

In summary, the progression of this project requires a multidisciplinary approach that draws on a range of methods and algebraic resources, as a solid understanding of electrochemistry, thermodynamics, transport phenomena and algebraic modeling is essential for designing, optimizing, and operating fuel cell systems that can meet the demands of urban mobility while reducing carbon emissions. Every equation and law employed to obtain the results presented over the next sections will be properly presented and discussed further in this report.

5. Key parameters

There are several factors influencing the performance of a PEMFC and it is important to be aware of the role they will play on the efficiency of the systems. Those parameters will guide the majority of analysis and discussions carried out on this report. One of the most important among those parameters is undoubtedly the membrane conductivity. It is a key component of PEMFCs, and its conductivity determines the transport of protons from the anode to the cathode. The membrane must have high proton conductivity to minimize the internal resistance of the fuel cell and maximize power output. A low conductivity can result in a high overpotential and decrease efficiency.[7] Therefore, selecting a membrane with high conductivity, low water uptake, and high chemical stability is important to improve the efficiency of PEMFCs.

The water management is another critical factor to maintaining the performance and durability of PEMFCs. The fuel cell must hold a proper water balance to ensure that the membrane is hydrated and that there is no flooding or drying. Too much water can lead to flooding, which reduces the effective surface area of the electrode and increases the resistance, while too little water can lead to drying, which reduces proton conductivity and increases the ohmic drop and the overpotential. Designing an effective water management system, such as a humidification system, is therefore essential to improve the efficiency of PEMFCs.

The tests carried out both in the experimental bench and the platform counted on a humidification system in order to assure the optimal operation on the fuel cell. In the experimental bench, the humification of the membrane was possible through a humidifier chamber filled by approximately half of its capacity. Water could be transferred from a water-supply vessel to the humidifier using a pump, and it was possible to increase the velocity of the transfer whenever the indication of water seemed to be decreasing below the desired level.

At the platform, the humidification was assured through a fuel cell humidifier humidifier chamber working on a counter current dynamic. The device is a *Px4-268* model, part of the *Px Series* from *dpoint humidifier*, and is designed to be a planar membrane humidifier for low pressures and low temperature applications. It contained a wet chamber through which the oxygen-depleted air leaving the fuel cell is meant to pass as well as a dry chamber in which the dry air stream entering the fuel cell should pass. This humidifier chamber will be the object of several analyses and is better represented in Figure 9.

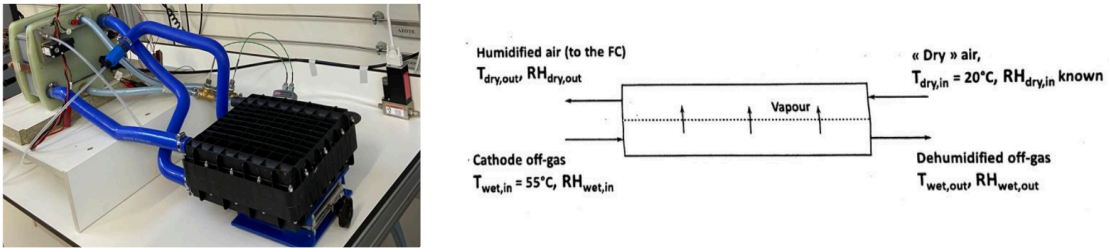

Figure 9: Photo and scheme of the humidifier chamber

Another important factor to be considered regards the catalysts, they are typically platinum-based and their activity plays a critical role in the efficiency of the fuel cell. Platinum is expensive and scarce, so researchers have been working to develop alternative catalysts that are more affordable and abundant. In addition, the catalysts must be highly active to speed up the reaction rate and maximize the conversion of fuel to electrical energy. A higher catalyst loading can improve activity, but it can also increase the cost and decrease durability.[15] Therefore, optimizing the catalyst composition, morphology, and loading is crucial to improve the efficiency of PEMFCs. The catalyst will not be one of the main objects of investigation in this report but their activity will have an influence over many considerations.

It is also crucial to acknowledge the operating temperature of PEMFCs as one of the parameters that can have a significant impact on their efficiency. The temperature must be optimized to ensure that the reaction kinetics are favorable and that the membrane is not damaged. A higher temperature can improve the reaction rate and reduce the overpotential, but it can also increase the risk of membrane degradation and reduce the durability of the fuel cell. A lower temperature can reduce the risk of membrane degradation, but it can also reduce the reaction rate and increase the overpotential. Therefore, selecting an appropriate operating temperature and designing a temperature control system is essential.

Lastly, the design and construction of the cell can also affect the efficiency of PEMFCs. The electrodes must have a high surface area to maximize the reaction rate and minimize resistive losses, while the cell must be constructed to minimize the contact resistance between the components. In addition, the thickness and porosity of the GDL can affect the transport of reactants and products. The design of the current collectors and flow channels can also affect the distribution of reactants and products, as well as the hydrodynamics of the system.

6. Tests on the 5 cell stack bench and results

This section will investigate the performance and characteristics of the PEMFC on the 5 cell stack experimental bench, providing a comprehensive overview as well as the significant outcomes obtained from the tests conducted on this system.

- Flowrates

The first step of this test was to calculate the flowrate of hydrogen and oxygen entering the system based on the monitored current. The values of current passing through the fuel cell varied in the range of 6,0 A to 26,0 A in steps of +0,5 A (thus 6,0; 6,5; 7,0…). This range was chosen due to certain constraints that do not allow it to work in high values of current, such as insufficient hydrogen inlet or the rising of the temperature of the fuel cell. The Faraday law was employed to calculate the molar flowrate which could then be converted to volumetric flowrate.

$$I = n_e \times F \times \dot{n}_{H2} \quad (4)$$

Where I, n_e, F and $\dot{n}_{H2}$ represent respectively the current, the number of electrons involved in the reaction normalized to 1 mol of the target molecule (in this case H_2), the Faraday constant and the molar flowrate. It is then possible to isolate the flow rate which will provide us with the relation indicating the flow rate going through a single cell in stoichiometric conditions. Since the number of cells N in the stack is bigger than 1 and the reactants are not in stoichiometric conditions but in excess - in order to assure the proper functioning of the fuel cell - those variables must also be taken into account. The excess is expressed by the stoichiometric ratio λ which indicates the ratio between the actual provided flowrate and the flowrate in stoichiometric conditions. The relation would then turn into:

$$\dot{n}_{H2} = N \times \frac{I \times \lambda}{n_e \times F} \quad (5)$$

The same process can be applied to oxygen in order to calculate the air flowrate.

$$\dot{n}_{air} = N \times \frac{I \times \lambda}{n_e \times F \times y_{O2}} \quad (6)$$

The new term y_{H2} is the molar ratio of oxygen in the air which is considered to be 21%. The value for N in the stack concerned equals 5, which will be therefore the value used to perform the calculation, but other assemblies might have distinct values. The number of electrons liberated/consumed is equal to 2 for hydrogen and to 4 for oxygen. Considering the stoichiometric ratios equal to $\lambda_{H2} = 1,2$ and $\lambda_{air} = 2,5$, the results are obtained and a selection of values (for the minimum, intermediate and maximum applied current) is shown to better illustrate the evolution. It is however important to notice that the results shown below do not

correspond to the actual flow rate at the laboratory conditions but rather at normal conditions (atmospheric pressure and 273,15K), which assures it to be safer to compare results regardless of daily variations in lab conditions.

Current (A)	Flowrate H2 (Ncm^3/min)	Flowrate air (Ncm^3/min)
6,0	251	747
15,0	627	1867
26	1087	3236

Table 2: flowrates for three selected current values for the 5 cell stack

The volumetric flowrate was easily obtained from the molar flowrate by manipulating the ideal gas law. Once the relation between flowrate and current was deduced from the Faraday law, thus denoting a first order correlation, the correlation observed between the parameters was rather expected.

- Voltage and power

The next step of the analysis concerns the establishment of a correlation between the voltage and electrical power of the fuel cell with the intensity of current. This will be achieved through the measurement indicated by the voltmeters and the software SPACE. The voltage of the stack, as well as the maximum, minimum and average voltage of the cells individually, are computed for the range of 25,0 A to 50,0 A at first. The range of currents employed for this test is different from the last experiment which monitored the flowrate because it was noticed that the voltage was not quite stable at lower figures, leading to the choice of higher current values. The stoichiometric factors were kept as $\lambda_{H2} = 1,2$ and $\lambda_{air} = 2,5$. The electrical power can then be calculated directly from the correlation $P = U \times I$. Both the table and the plots are represented below for better visualization.

		(Volts)				
Current (A)	Temperature of fuel cell (ºC)	Min	Aver	Max	U (stack)	Power (W)
50	57	0,512	0,559	0,603	2,802	140,1
45	58	0,530	0,584	0,623	2,924	131,58

40	57,5	0,574	0,606	0,638	3,031	121,24
35	57	0,610	0,632	0,659	3,155	110,425
30	54,9	0,643	0,653	0,673	3,273	98,19
25	54,7	0,655	0,670	0,691	3,352	83,8

Table 3: computed values of individual voltages for a range of current intensity

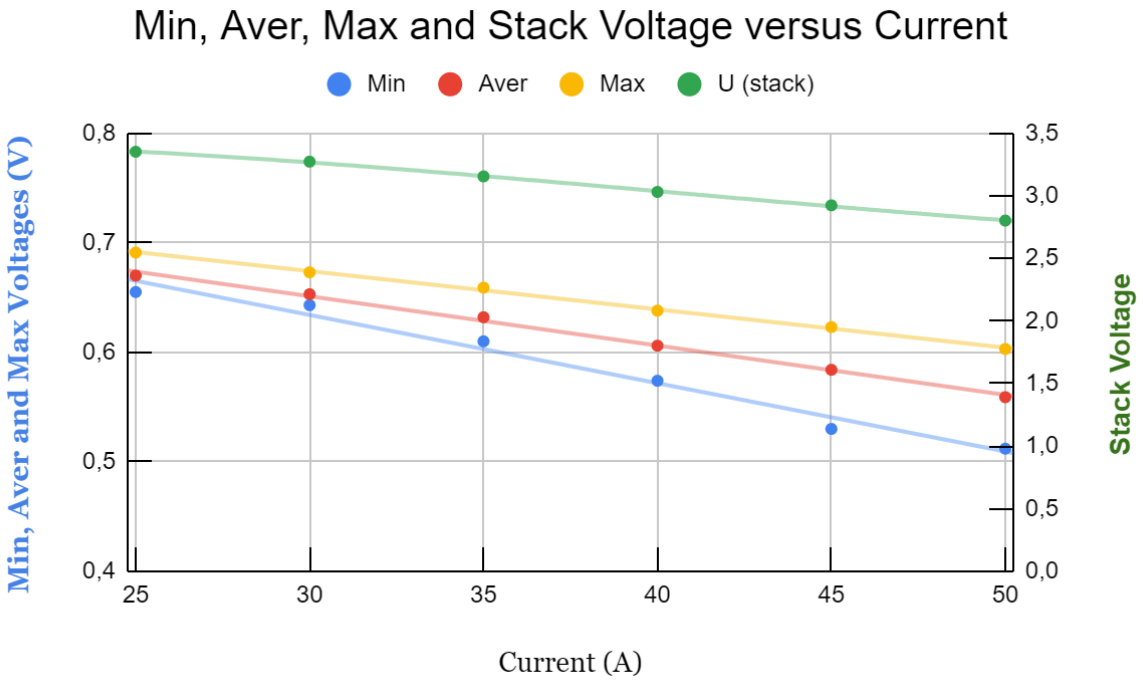

Figure 10: polarization curve for the first tests at the experimental bench

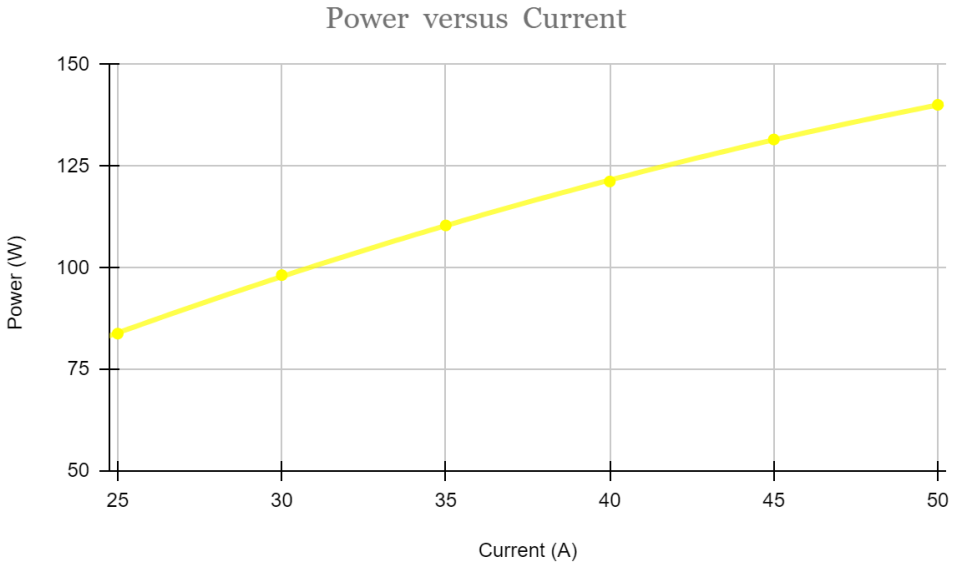

Figure 11: power generated by the fuel cell versus the current intensity

The same experiment was repeated on the experimental bench a couple months later in order to investigate any differences. This time however, the stoichiometric factor was higher for both reactants (λ_{H2} went from 1,2 to 2,0 and λ_{air} from 1,5 to 3,0). Despite some potential instability in the data monitoring, it was decided to carry out the experiment at lower currents as well. To minimize instability, imprecision, and ensure optimal fuel cell performance at lower currents, the following procedure was implemented:

1. The experiment was initiated at 30.0 A and conducted until 50.0 A (same range as before).
2. The system was then set back to 30.0 A and ran until it stabilized at the same temperature recorded during the initial 30.0 A stage.
3. The experiment was conducted now from 30,0 A until the 0,0 A (OCV).

This procedure enables the fuel cell to operate at a higher performance level before reducing the current to 30.0 A and below. By running the experiment for a longer duration and at higher currents, the fuel cell achieves a desired level of humidification and temperature that would be difficult to reach if initiated directly at low currents. Consequently, the fuel cell functions more appropriately and exhibits fewer oscillations under these conditions. Stabilizing the system at the same initial temperature it had at 30.0 A is crucial for test accuracy and achieving a steady state, thus enhancing result precision. The open circuit voltage (OCV) refers to the potential difference across the stack when there is no current flowing through it. The results are shown below.

		Volts				
Current (A)	Temperature of the fuel cell (ºC)	Min	Aver	Max	U (stack)	Power (W)
OCV	54,3	0,962	0,969	0,98	4,85	-
1,5	54,3	0,871	0,874	0,88	4,371	6,56
5	54,4	0,815	0,821	0,83	4,106	20,53
10	54,6	0,759	0,773	0,79	3,87	38,66
15	54,7	0,725	0,737	0,75	3,69	55,29
20	54,9	0,68	0,697	0,71	3,49	69,8
25	55,1	0,65	0,678	0,7	3,39	84,73
30	55,3	0,613	0,648	0,68	3,25	97,44
35	55,4	0,583	0,624	0,66	3,12	109,2

40	55,8	0,551	0,601	0,65	3,0	119,96
45	56,8	0,508	0,573	0,621	2,873	129,29
50	57,9	0,452	0,541	0,6	2,69	134,5

Table 3: recorded values of individual voltages for a range of current intensity

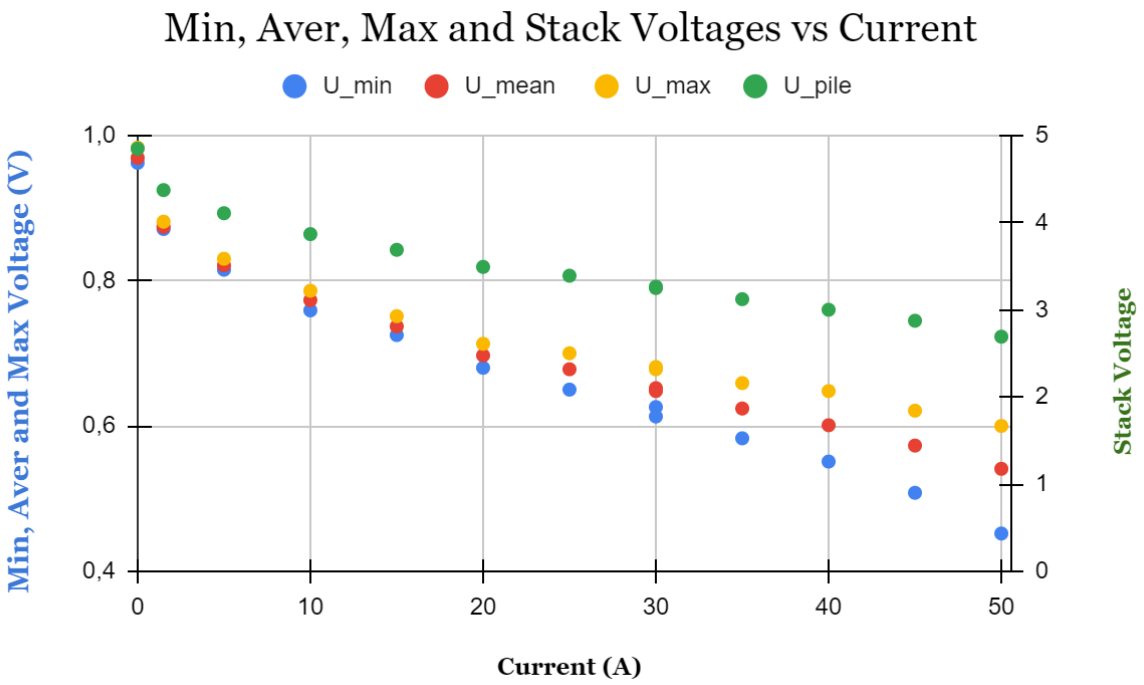

Figure 12: polarization curve for the first tests at the experimental bench

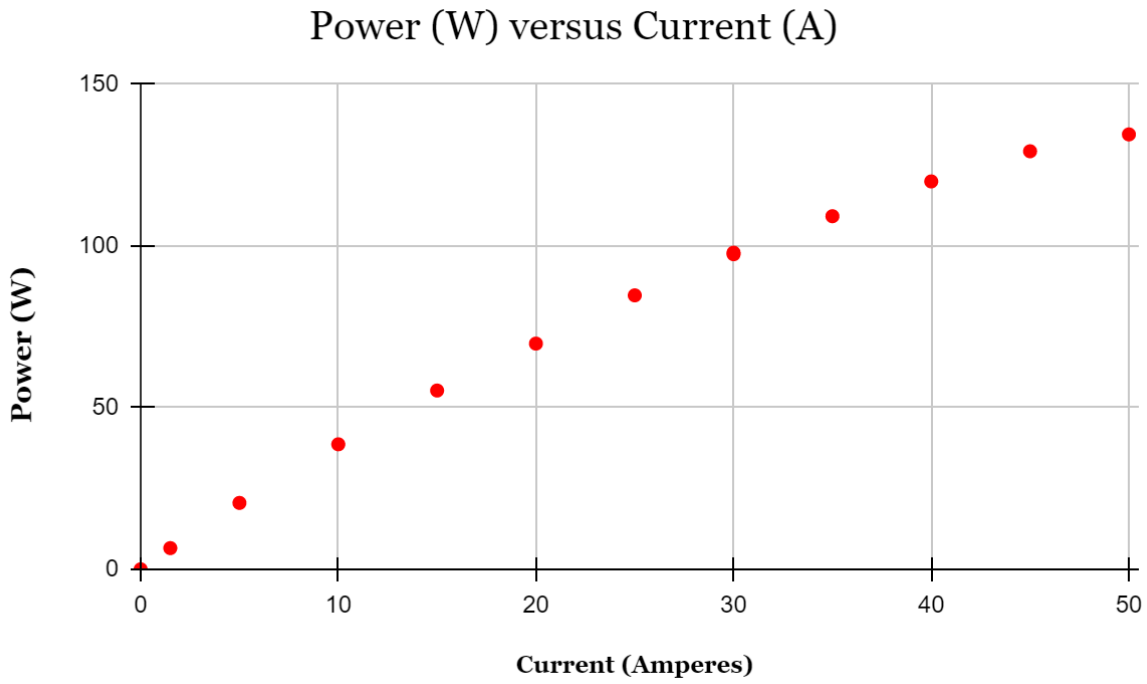

Figure 13: power generated by the fuel cell versus the current intensity

It is possible to note that the performance of the fuel cell was slightly worse at the second experiment. The performance drop was not very significant for the moderate currents, starting at only about 0,8% for 30,0 A, but it increased for higher values being as critical as about 4% for 50,0 A. The experiments were not carried out in exactly the same conditions, the main difference being indeed the stoichiometric factor which was considerably higher compared to the first time and for which the influence on the results will be investigated in the next section. The performance drop might also be explained by other factors such as the water content and management, temperature or even the aging of the fuel cell which can lead to a lower catalyst activity or worse hydrodynamics.

- Stoichiometric factor

The stoichiometric factors, represented by the ratio of reactants, play a crucial role in determining the efficiency, stability, and output characteristics of the fuel cell. Through experimental analysis and data interpretation, these tests aim to shed light on the relationship between stoichiometry and fuel cell performance.

- Hydrogen

The stoichiometric factor of hydrogen was kept between a narrower range of values compared to the stoichiometric factor of air. Nevertheless, it was possible to observe that a larger stoichiometric factor of hydrogen yields increased voltages and consequently, higher power output for the same current. For the test below, the stoichiometric factor of air was kept constant (λ_{air} = 3,0) and while that of hydrogen was varied (λ_{H2} = [1,2; 1,3; 1,4; 1,5]).

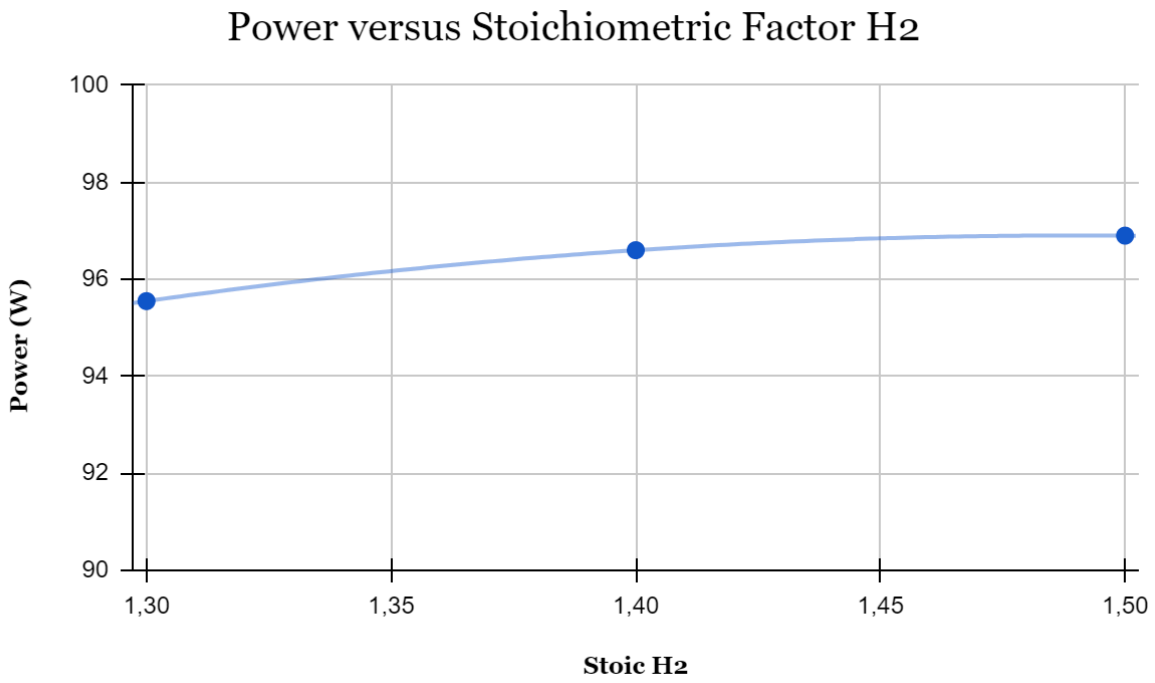

Figure 14: Power generated in the 5 cell stack versus stoichiometric factor of hydrogen

It was observed that the system was able to generate more power for higher stoichiometric factors and, for λ_{H2} = 1,2 or lower, the system presented high instability.

- Air

Higher stoichiometric factors for air were also beneficial for the fuel cell performance. For the test presented below, the stoichiometric factor of hydrogen was kept constant at λ_{H2} = 1,5 whereas that of air was varied (λ_{air} = [2,9; 2,8; 2,7; 2,6; 2,5]).

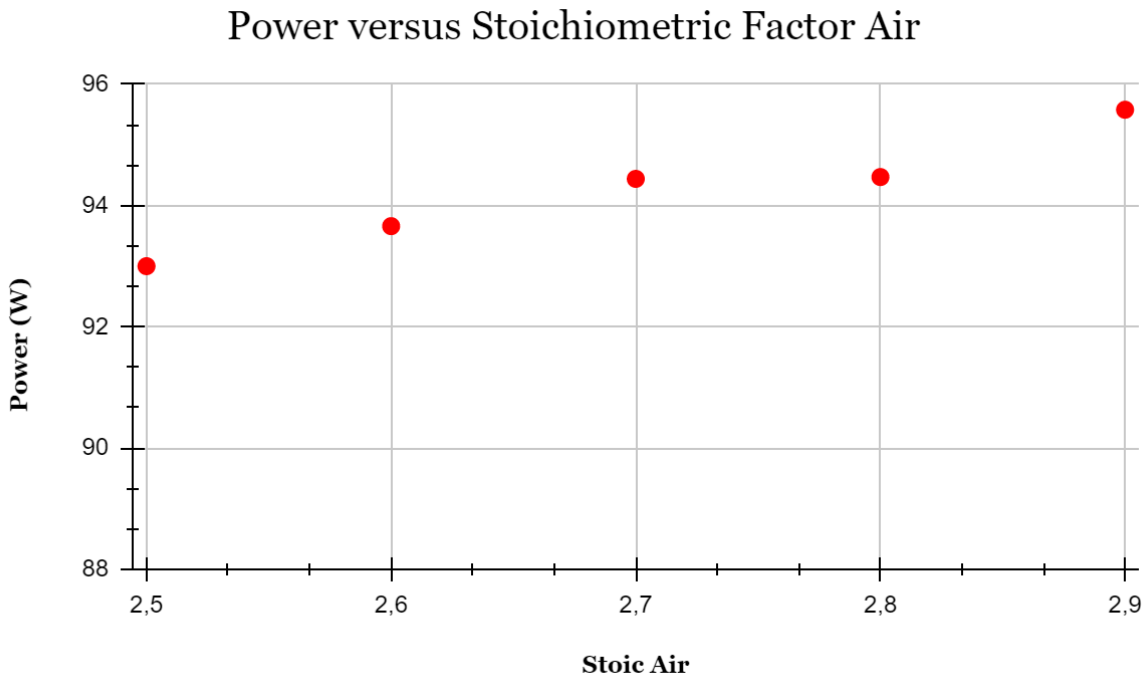

Figure 15: Power generated versus stoichiometric factor of air

It would be consequently interesting to increase the stoichiometric factor of air in order to obtain better outputs. Besides having a direct contribution to the energy generated, an excess of air also helps to evacuate heat. Air is also cheaper than hydrogen as a reactant so increasing the air consumption would generally represent a lower cost compared to doing the same operation with hydrogen.

7. Tests on the platform and results at low currents

Initially, the platform did not dispose of a flowmeter capable of providing a large hydrogen flowrate, which means that it would not be possible to reach the required hydrogen intake to generate larger currents. The system was equally not equipped with a cooling system, meaning that the rising of the temperature could not be controlled properly in case large amounts of heat were being generated. Therefore, at a first moment, the tests were carried out for low and moderate currents. This section will describe the tests realized during the absence of the high capacity flowmeter and the cooling system.

- Voltage and power

In parallel to the experimental bench, test measurements were initially performed on the platform's fuel cell to analyze the correlation between current, voltage and power. The results of the tests are represented below for the range of currents from 1,0 A to 14,0 A along with the graph describing this correlation.

	I (A)	U (V)	P (W)
flowrate H_2 5L/min flowrate air 20L/min	0,97	60	58,2
	1,98	59,3	117,414
	3	58,1	174,3
	4	57,5	230
	5,01	57	285,57
	6,02	56,4	339,528
flowrate H_2 8L/min flowrate air 40L/min	6,02	57,4	345,548
	7,03	56,56	397,6168
	8,03	56,59	454,4177
	8,96	56,3	504,448
	9,965	56	558,04
	10,97	55,6	609,932
	11,98	55,2	661,296
	13	54,8	712,4
	14	54,2	758,8
pronounced fall on system's voltage	15	52,1	781,5

Table 4: results of the first test at the H_2 platform (70 cell stack, Symbio)

The test did not go forward after 15,0 A because in addition to the absence of a cooling system mentioned before, the voltage began to decrease significantly at this point. This is most likely due to the possibility of not having a hydrogen flowrate elevated enough to create an intensity of current that could go beyond 15,0A. It was already acknowledged that 15,0 A would be close to the limit because the hydrogen has a stoichiometric constant, in standard cubic centimeters per min, of around 7,0 Ncm^3 per cell per minute to produce 1 mol of

current at standard state conditions. It means that the volume required to create 15,0 A for a stack of 70 cells would be around 7,35 L/min assuming a total conversion.

$$15,0\,A \;=\; \frac{(required\ flowrate)}{(7{,}0\ NmL/cell/Ampere)\times(number\ of\ cells)} \;\Rightarrow\; required\ H_2\ flowrate \;=\; 7,35\ NL/min$$

A stoichiometric factor greater than 1,0 is crucial for the hydrogen inlet in order to ensure a reliable operation and no starvation of the fuel cell outlet.[10] For most tests, a factor of $\lambda_{H2} = 1,2$ was chosen so that the reaction could run as desired throughout the integrity of the fuel cell. The hydrogen flowrate of 8,0 L/min is therefore probably not enough to avoid the fatigue of the fuel cell due to the lack of reactants, as it is quite close to the requirement.

Besides, the small excess of hydrogen leaving the cell could prevent the proper expel of the water contained in the anode, risking the flooding of the anode compartment and leading then to a poor performance. Due to this sudden voltage drop, it was decided that the values attributed to 15,0A should be disconsidered for the plot in the sake of better precision.

Another interesting phenomena to be observed in the primary computed results is the slight change in the voltage as the flowrates change and the setup current density is kept the same. More precisely, for the current at 6,02 A, the hydrogen and air flowrates went up from 5,0 NL/min to 8,0 NL/min and 20 NL/min to 40,0 NL/min respectively. The voltage increased then from 56,4 V to 57,4 V - an increase of about 1,7% for the same current intensity.

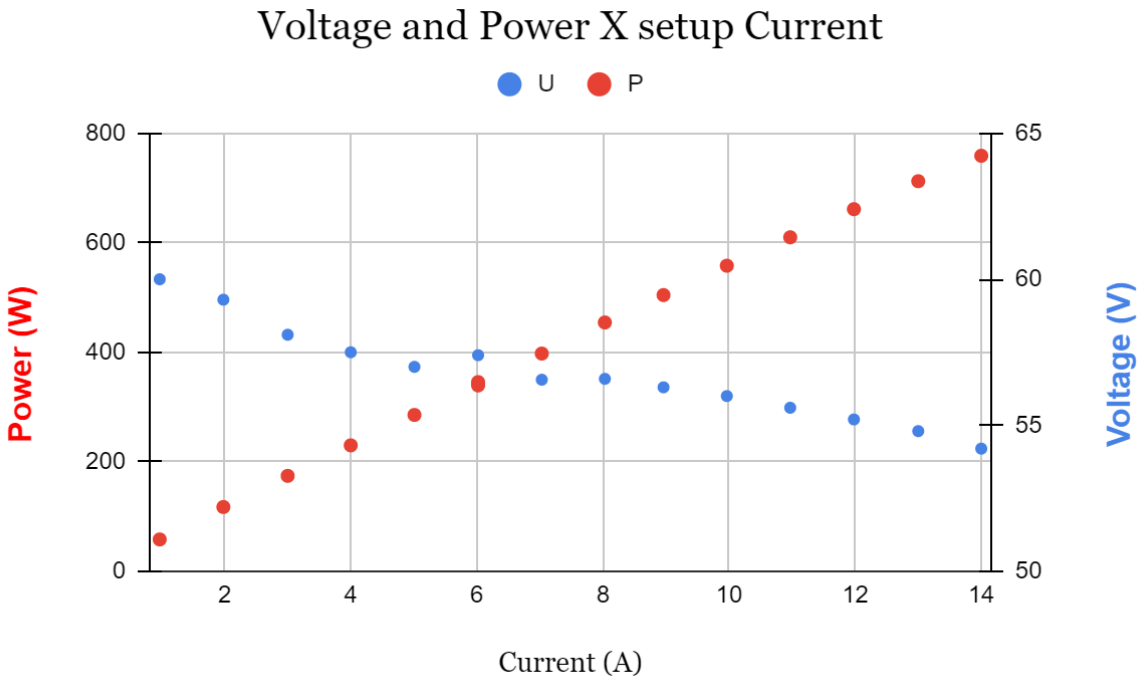

Figure 16: corresponded power and voltage for each current intensity set

- Heat

One of the important features of the fuel cell to be understood is the heat release. It is of general knowledge that real energy generators cannot present an efficiency of 100%. The efficiency of PEMFCs is often highlighted because, since it does not constitute a heat engine, its efficiency is not limited to the Carnot's cycle. There exists however losses related to mass and charge transfer, which are represented by an entropy term. The theoretical maximum efficiency of a fuel cell η_{max}, also called 'thermodynamic efficiency' is represented by:

$$\eta_{max} = \frac{\Delta G}{\Delta H} \tag{7}$$

This ideal efficiency is usually in the region of 85% at environmental temperature.[7] Operating at the maximum theoretical performance, the cell would equally present a maximum theoretical voltage, also known as open circuit voltage. It is defined by the voltage observed when the system is thermodynamically reversible. There are nevertheless thermodynamic energy losses yet to be considered, related for example to ohmic drop or activation polarization.[7] These energy losses are dissipated in the form of heat, which will be estimated in this section.

In order to perform the calculation, the values of HHV will be employed, therefore taking into account the enthalpy of combustion of the fuel and including the heat released by condensing the water vapor formed during combustion.[5] The voltage of a fuel cell if all the energy from the hydrogen fuel was transformed into electrical energy would be given by:

$$U_{reference} = \frac{\Delta h_r}{2F} \tag{8}$$

Where Δh_r is the enthalpy of the reaction generating water from hydrogen and oxygen. The factor two multiplying the Faraday number is due to the fact that for each mol of water produced, two electrons are liberated in the oxidation of hydrogen, thus forming the electrical current. The reaction enthalpy here is equal to -285,84 kJ - corresponding, as stated before, to the higher heating value (HHV) at standard conditions. The relation between the enthalpy-based voltage and the computed voltage express a link to the efficiency of the fuel cell and therefore the dissipated heat. The value for $U_{reference}$, also known as thermoneutral voltage, is then obtained, being around 1,48 V. It can be plotted along with the average computed voltage for each cell over the current intensity.

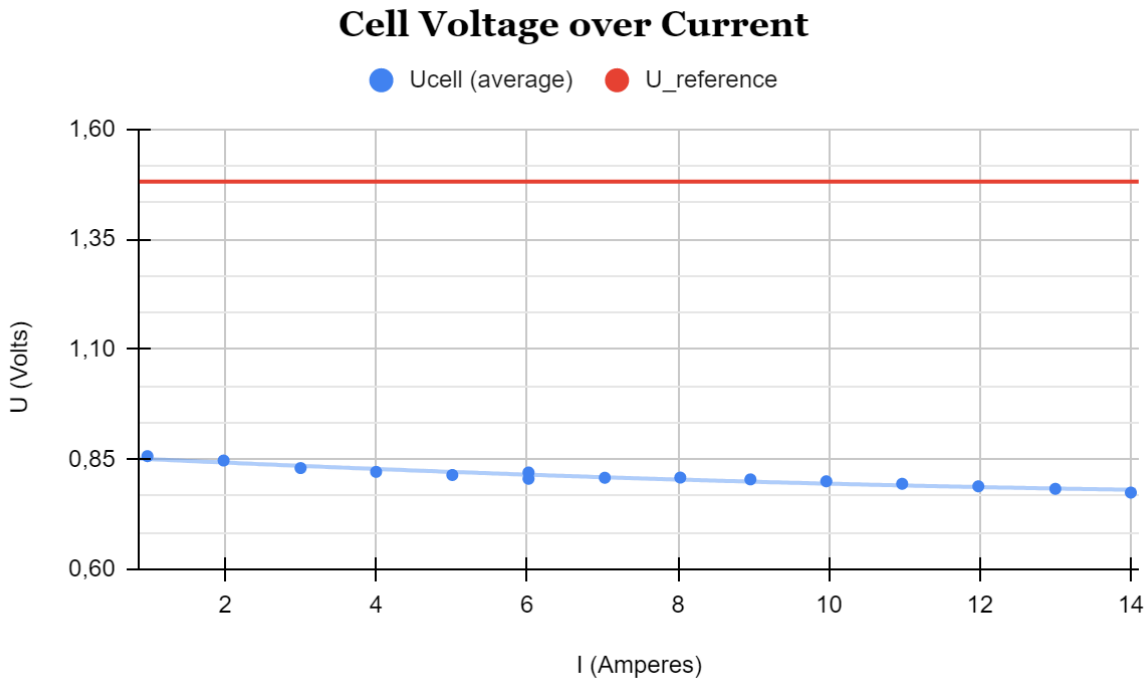

Figure 17: reference voltage based on enthalpy and measured voltage of a single cell over current

It is possible to notice that, as the current increases, the average potential for each cell will decrease as the reference potential is constant. By multiplying both by the current, the former will give the total amount of energy created by the fuel cell, and the latter will express the energy that is actually converted into electrical energy. The difference between those two parameters would give the dissipated heat per cell. It is then possible to obtain the heat generated by the whole system by multiplying this value by the number of cells.

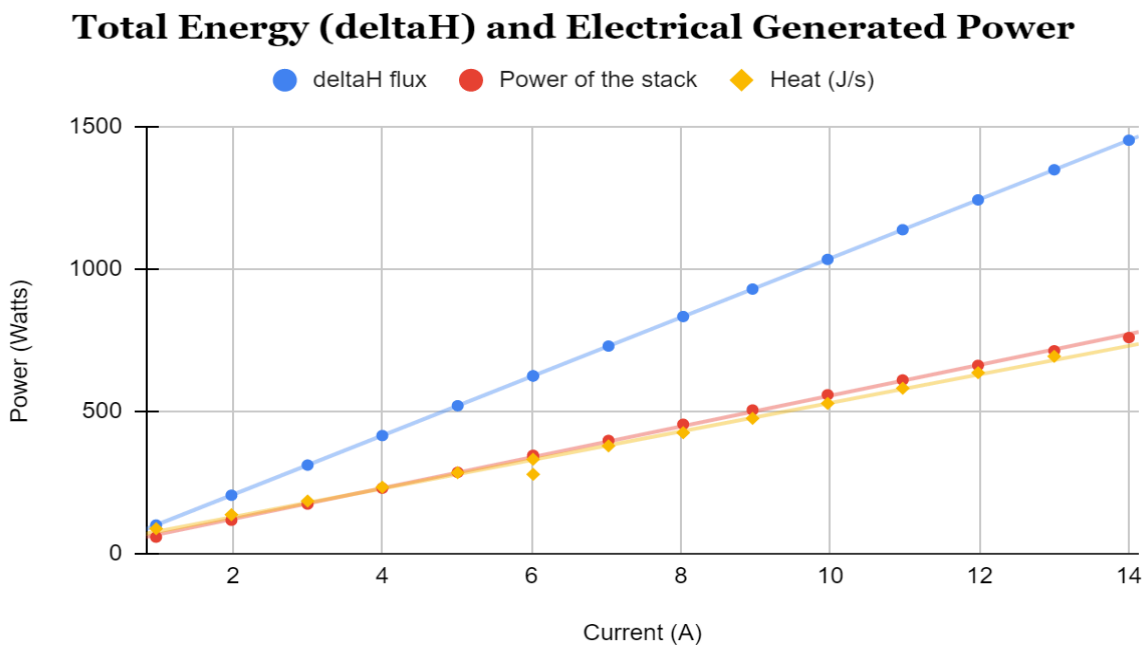

Figure 18: dissipated heat over current

It is possible to observe that for a current of 15,0 A, the system would be dissipating around 750 W. It is a quite expressive amount of heat to be dealt in the absence of a cooling system, which might help to explain the reason of the system being shut down at this point following the sudden voltage drop.

- Humidity

The next aspect to be investigated on the system will be the humidity. The purpose of having some humidification into the system is that the proton conductivity through the membrane relies on a sufficient content of water on the polymer electrolyte. It is however a tricky parameter because, whereas a certain level of humidity is essential to assure the well

functioning of the fuel cell - specially for the gas/oxygen inflow - an excess of humidity might lead to the formation of liquid water, which can lead to the flooding of the catalyst layer or even the gas diffusion layer.[7]

Before digging into the aspects surrounding humidification, it is recommendable to better understand the equations and the mass balance on the system of the fuel cell. The equationing will be developed based on the cathode electrode:

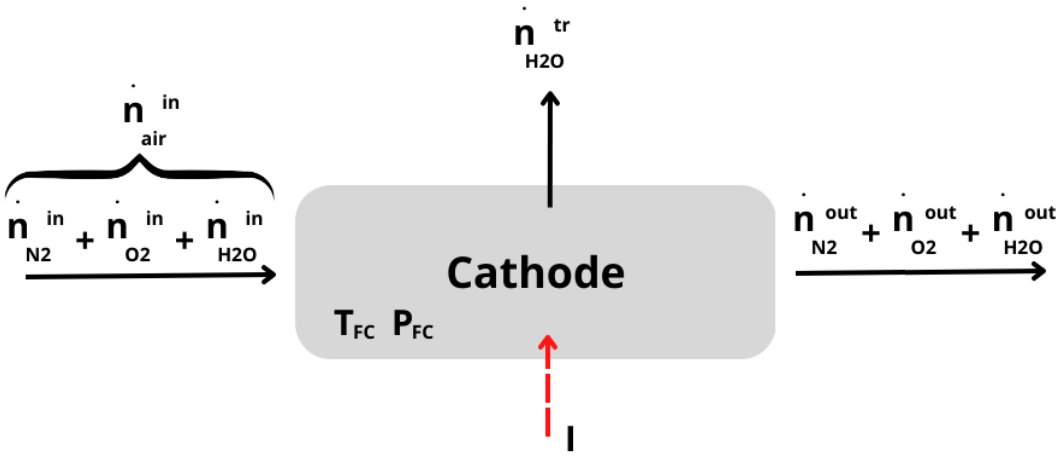

Figure 19: mass balance around the cathode subsystem

For further analysis, the air entering the cathode will be composed of nitrogen, oxygen and water. The ratio for oxygen and nitrogen will always be the same in dry air (21% and 79%), whereas the water flowrate entering the system will vary as a function of the relative humidity (RH). The nitrogen flowrate will always be the same whether it is entering or leaving the cathode as it does not participate in the reactions ($\dot{n}_{N2}^{in} = \dot{n}_{N2}^{out}$). The oxygen will be consumed in the cathode ($\dot{n}_{O2}^{in} \succ \dot{n}_{O2}^{out}$) whereas water will be generated ($\dot{n}_{H2O}^{in} \prec \dot{n}_{H2O}^{out}$). A fraction of the water in the cathode might be transferred to the negative electrode ($\dot{n}_{H2O}^{tr}$). I, T_{FC} and P_{FC} represent respectively the current running through the cathode, the temperature of the fuel cell and the pressure of the fuel cell.

In this section, three scenarios were studied: (i) dry air with no water transfer between the electrodes, (ii) moist air with no net water transfer between the electrodes and (iii) moist air

with water transfer between the electrodes. The three scenarios and the algebraic development for each one are detailed further in this section.

(i) **Dry air, no water transfer to the anode**

The equations for molar rates are deduced from the Faraday law and mass balances.

Cathode:

$$\dot{n}_{O2,\,consumed} = N \times \frac{I}{4F} \tag{9}$$

$$\dot{n}_{H2O,\,produced} = N \times \frac{I}{2F} \tag{10}$$

$$\dot{n}_{O2}^{\,in} = N \times \lambda_{O2} \times \frac{I}{4F} \tag{11}$$

$$\dot{n}_{air}^{\,in} = N \times \frac{\lambda_{O2}}{y_{O2}} \times \frac{I}{4F} \tag{12}$$

$$\dot{n}_{N2}^{\,in} = \dot{n}_{air}^{\,in} - \dot{n}_{O2}^{\,in} \tag{13}$$

Outlet:

$$\dot{n}_{N2}^{\,out} = \dot{n}_{N2}^{\,in} \tag{14}$$

$$\dot{n}_{O2}^{\,out} = \dot{n}_{O2}^{\,in} - N \times \frac{I}{4F} \tag{15}$$

$$\dot{n}_{H2O}^{\,out} = N \times \frac{I}{2F} \tag{16}$$

Final mass balance:

$$\dot{n}_{total}^{\,out} = \dot{n}_{H2O}^{\,out} + \dot{n}_{N2}^{\,out} + \dot{n}_{O2}^{\,out} \tag{17}$$

It is then possible to calculate the relative humidity (RH), which is the ratio between the molar ratio of water leaving the cell and the molar ratio of water in saturated conditions. The former can be obtained by dividing the flowrate rate of water leaving the fuel cell while the latter can be found through the pressure of saturation using either Buck's (18) or Antoine's (19) equation.

$$P_{H_2O}^{sat} = \ 0,6112\ exp\left(\left(18,678 - \frac{T}{234,5}\right)\left(\frac{T}{257,14+T}\right)\right) \tag{18}$$

$$\log_{10} p = A - \frac{B}{C+T}. \tag{19}$$

The temperature shall be employed in ºC for Buck's or in Kelvin for Antoine's equation. The Buck's equation was used because it is the most precise for the range of temperatures observed in the fuel cell. If Antoine's equation was chosen instead, the coefficients for A, B and C are respectively 5,20389, 1733,926, -39,485.[8] Final equations after development of all algebraic terms will therefore be:

$$y_{H2O}^{\ out} = \frac{n_{H2O}^{\cdot\ out}}{n_{total}^{\cdot\ out}} = \frac{2}{1+\frac{\lambda_{O2}}{y_{O2}}} \tag{20}$$

$$y_{H2O}^{sat} = \frac{P_{H2O}^{sat}}{P^{fuel\ cell}} \tag{21}$$

$$RH = \frac{2 \times P^{fuel\ cell}}{P_{H2O}^{sat} \times (1+\frac{\lambda_{O2}}{y_{O2}})} \tag{22}$$

An example of the calculation for this scenario can be seen in the excel spreadsheet below, where some of the parameters were assumed in order to allow the reasoning upon the scenario.

Relative humidity calculation, dry air

Data		
Faraday number	96485	C/mol
T_fuel_cell	55	°C
lambda O2	2,5	-
I	10	A
nº of cells in the stack	70	-
P_fuel_cell	1,01	bar

Cathode		
n_O2_consumed	1,81E-03	mols
n_H20_produced	3,63E-03	mols
n_in_O2	4,53E-03	mols
n_in_air	2,16E-02	mols
n_in_N2	1,71E-02	mols
Outlet		
n_out_N2	1,71E-02	mols
n_out_O2	2,72E-03	mols
n_out_H2O	3,63E-03	mols
n_out_total	2,34E-02	mols

Assumption 2: all the components are in gas form			
y_out_H20	1,55E-01	-	
Psat	15,76	kPa	Buck equation
Psat	0,158	bar	
y_sat_H2O	1,56E-01	-	
if y_out_H2O<y_sat_H2O then assumption 2 is true			
Conclusion	1,56E-01	green -> true, red -> false	
RH_out	0,99	-	

Figure 20: data and results for the first scenario

It is equally important to acknowledge that this scenario is not realistic, as even for an extremely dry atmosphere, the relative humidity of the air entering the system would not be nil. Despite this, the first scenario helped to develop the following two with a more solid base.

(ii) **Moist air, no water transfer to the anion**

The reasoning was very similar to the first case, as the single difference is that the air entering the system now has a certain degree of water content. For a given relative humidity RH, it is possible to calculate the molar fraction of water in the air entering the chamber through the equation $RH = \frac{y_{H2O}^{air,in}}{y_{H2O}^{sat}}$. The molar fraction of water in saturation conditions depends critically on the temperature, and might be obtained simply by applying by rearranging the equation (20), providing Raoult's law $P^{sat} = y_{H2O}^{sat} \times P$.

The partial pressure of water is tabled and its values are extracted into a spreadsheet in order to automatize the obtention results. Once the molar fraction of water entering the chamber is obtained, it is simple to modify the equations based on the new configuration. The air will contain a fraction $y_{H2O}^{air,in}$ of water, and the rest will be composed of oxygen and nitrogen in the same proportion as in the last case. The water leaving the fuel cell will no longer be equal to the water produced either, but to the sum of it with the water content of the air. The final equations for the fraction of water leaving the fuel cell and the relative humidity at the exit will therefore be:

$$y_{H2O}^{out} = \frac{\frac{\lambda_{O2}}{y_{O2}(1-y_{H2O}^{in})} y_{H2o}^{in} + 2}{\frac{\lambda_{O2}}{y_{O2}(1-y_{H2O}^{in})} + 1} \tag{23}$$

$$RH_{out} = \frac{\frac{\lambda_{O2}}{y_{O2}(1-y_{H2O}^{in})} y_{H2o}^{in} + 2}{\frac{\lambda_{O2}}{y_{O2}(1-y_{H2O}^{in})} + 1} \times \frac{P^{fuel\ cell}}{P_{H2O}^{sat}} \tag{24}$$

The water leaving the fuel cell will no longer be equal to the water produced either, but to the sum of it with the water content of the air.

It is expected that, for this scenario, the probability of flooding increases as more water gets accumulated in the cathode electrode. For the results presented below, it was notice that for the identical conditions of the first scenario (dry air), that being, at the fuel cell temperature

of 55ºC, a stoichiometric factor of 2,5 for oxygen and a current of 10,0 A, as well as an assumed relative humidity of 40%, some water would condensate. In order to avoid the flooding of the system, it is possible to slightly increase the temperature of the fuel cell. The content of water in the air in saturation conditions increases sensibly with the temperature, so by increasing the temperature in +1ºC only (T_{FC} = 56ºC) the problem is solved.

To the extent of ensuring a security margin for eventual oscillations, the temperature will be established at T_{FC} = 58ºC. Generally, the temperature shall not be increased to over 60ºC because it is the temperature where the rate of water production is the same as water being captured by the air, so nearly all the water produced will leave the system and the membrane is at risk of getting too dry - and therefore have is performance compromised.

Relative humidity calculation, humidified air

Data					
Faraday number	96485	C/mol	yH2O_sat_Tamb	0,023	-
T_fuel_cell	58	ºC	Patm	1	bar
lambda O2	2,5	-	yH2O_in	0,0092	-
I	10	A			
nº of cells in the	70	-			
P_fuel_cell	1,01	bar			
RH air	40	%	-> when Tamb is modified, modify manually the pressure according to the table there ->		
Tamb	20	ºC			

Cathode			
n_O2_consumed	1,81E-03	mols	
n_H20_produced	3,63E-03	mols	
n_in_O2	4,53E-03	mols	
n_in_air	2,18E-02	mols	
n_in_N2	1,71E-02	mols	1,71E-02
n_in_H2O	2,00E-04	mols	
Outlet			
n_out_N2	1,71E-02	mols	
n_out_O2	2,72E-03	mols	
n_out_H2O	3,83E-03	mols	
n_out_total	2,36E-02	mols	

Assumption 2: all the components are in gas form			
y_out_H20	1,62E-01	-	
Psat	18,17	kPa	Buck equation
Psat	0,182	bar	
y_sat_H2O	1,80E-01	-	
if y_out_H2O<y_sat_H2O then assumption 2 is true			
Conclusion	1,80E-01	green -> true, red -> false	
RH_out	0,90	-	

Figure 21: data and results for the second scenario

(iii) **Moist air, with some water transfer to the anode**

This is the general scenario, where the air entering the system contains water and part of the water produced in the cathode is transferred to the anode through the membrane, which means that the flowrate $n_{H2O}^{\cdot tr}$ in Figure 19 is not equal to zero as in the precedent cases. The ratio of water transferred to the anode will be denoted by:

$$\alpha = \frac{n_{H2O}^{\cdot tr}}{n_{H2O}^{\cdot prod}} \tag{25}$$

Where $n_{H2O}^{\cdot prod}$ represents the flowrate of water production in the cathode. The equation of the system will be identical to the second scenario regarding the entry flowrates. However, the water leaving the system will now be described by:

$$n_{H2O}^{\cdot out} = n_{H2O}^{\cdot in} + (1 - \alpha) \times n_{H2O}^{\cdot prod} \tag{26}$$

The final equations for the fraction of water leaving the fuel cell and the relative humidity at the exist will therefore be:

$$y_{H2O}^{out} = \frac{\frac{\lambda_{O2}}{y_{O2}(1-y_{H2O}^{in})} y_{H2o}^{in} + 2(1-\alpha)}{\frac{\lambda_{O2}}{y_{O2}(1-y_{H2O}^{in})} + 1 - 2\alpha} \tag{27}$$

$$RH = \frac{\frac{\lambda_{O2}}{y_{O2}(1-y_{H2O}^{in})} y_{H2o}^{in} + 2(1-\alpha)}{\frac{\lambda_{O2}}{y_{O2}(1-y_{H2O}^{in})} + 1 - 2\alpha} \times \frac{P^{fuel\ cell}}{P_{H2O}^{sat}} \quad (28)$$

In order to proceed with the calculation, it was assumed that the 10% of the water produced in the cathode was transferred to the anode ($\alpha = 0,1$). This value is coherent once the ratio of water transfer to the anode varies in the range of 5% to 30% in normal conditions.[7] The remaining conditions of temperature, pressure and current were set to be identical to the first scenario. The relative humidity was set at 40%. The following results are obtained:

Relative humidity calculation, humidified air and water transfer to the anode

Data					
Faraday numbe	96485	C/mol	yH2O_sat_Tamb	0,023	-
T_fuel_cell	55	ºC	Patm	1	bar
lambda O2	2,5	-	yH2O_in	0,0092	-
I	10	A	α (water transfer coef)	0,1	
nº of cells in the	5	-			
P_fuel_cell	1,01	bar			
RH air	40	%	-> when Tamb is modified, modify manually the pressure		
Tamb	20	ºC	according to the table there ->		

Cathode		
n_O2_consume	1,30E-04	mols
n_H20_produce	2,59E-04	mols
n_in_O2	3,24E-04	mols
n_in_air	1,56E-03	mols
n_in_N2	1,22E-03	mols
n_in_H2O	1,43E-05	mols
Outlet		
n_out_N2	1,22E-03	mols
n_out_O2	1,94E-04	mols
n_cat_H2O	2,59E-05	mols
n_out_H2O	2,48E-04	mols
n_out_total	1,66E-03	mols

Assumption 2: all the components are in gas form		-> to be tested
y_out_H20	1,49E-01	-
Psat	15,76	kPa
Psat	0,158	bar
y_sat_H2O	1,56E-01	-

if y_out_H2O<y_sat_H2O then assumption 2 is true		
Conclusion	1,56E-01	green -> true, red -> false
RH_out	0,96	-

Buck equation

Figure 22: data and results for the third scenario

8. Tests on the platform and results at higher currents

- Voltage and Power

The tests were carried out keeping the stoichiometric factor constant (λ_{H2} = 1,2 and λ_{air} = 2,5) for both hydrogen and oxygen in order to neutralize its influence on the performance of the fuel cell. Besides the current and the voltage, the temperatures of the fuel cell and the cooling cycle were also monitored.

Current (A)	Voltage (V)	T1 FC (in)	T2 FC (out)	T1 cooling (in)	T2 cooling (out)	Power (kW)
10	54,5	54,6	55,5	53,8	52,7	0,5
15	53,4	54,6	56,4	51,8	47,4	0,8
20	51,3	54,5	56,8	51,8	46,7	1,0
25	50,1	54,6	57,3	50,4	43,2	1,3
30	49,8	52,1	55,9	48,2	39,3	1,5
35	49,3	49,8	54,1	45,7	36,7	1,7
40	48,5	51,7	56,6	47,8	38,2	1,9
45	48,2	51,1	56,6	47,2	36,9	2,2
50	47,7	52,4	58,7	48,9	38,1	2,4
55	46,6	52,4	59,4	48,9	37,3	2,6

Table 5: results of the first test at the H_2 platform (70 cell stack, Symbio)

The limitation for this test was not the cooling system or the flowmeter anymore, but the load which had the capacity of absorbing around 2,5 kW, and the boundary is reached for the current I = 55,0 A. It is observed that the outlet temperature of the fuel cell generally increased over the tests for higher values of current. In order to compensate for the temperature rise, the number of fans as well as the intensity of their operation in the cooling system were adjusted along the experiment to evacuate more heat.

The polarization curve of the 70 stack fuel cell for this test is represented below. To generate around 2,5 kW at the boundary at 55,0 A, the flowrates of hydrogen and air were respectively 32,2 Nl/min and 160 Nl/min.

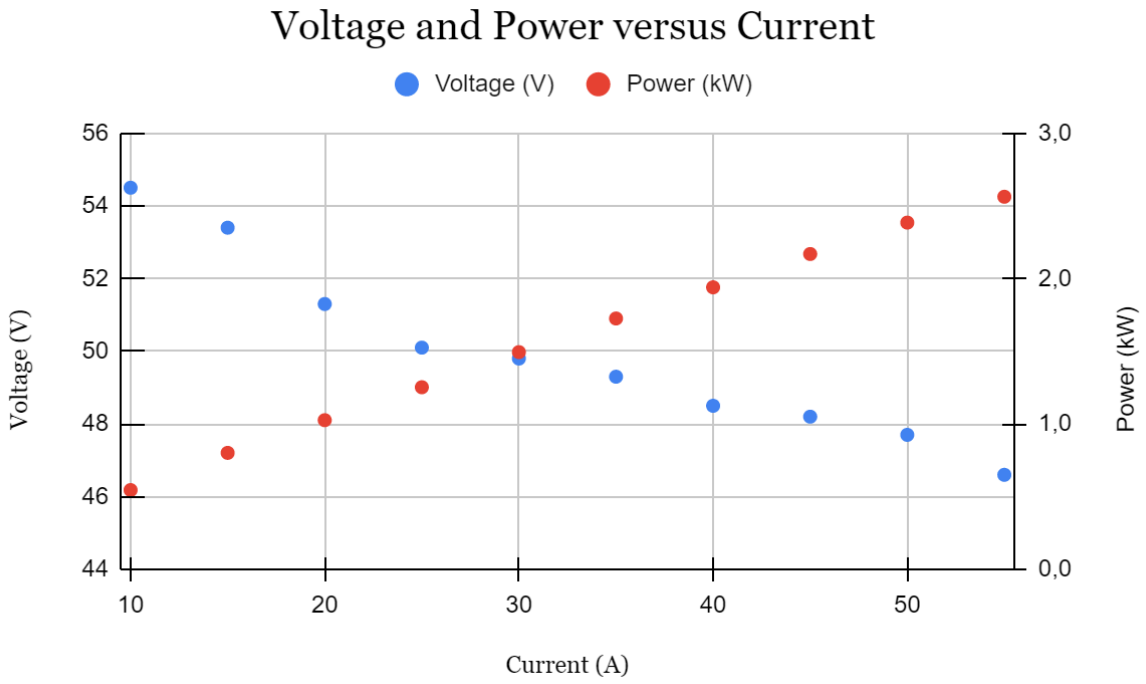

Figure 23: Voltage and power over current for the 70 cell stack

The cell voltage distribution was also monitored during the experiment. For the highest value of current (55,0 A), the voltage of each cell starting from the converter is illustrated.

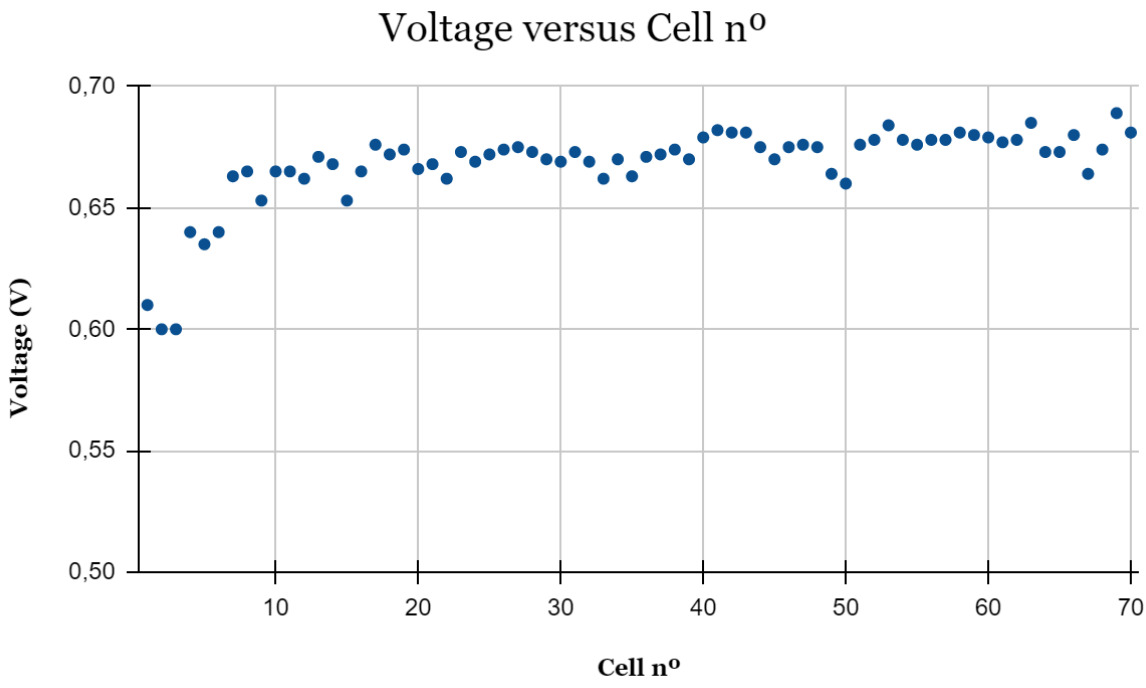

Figure 24: Voltage distribution for the 70 cell stack (cell 1° is the closest to the converter and so on)

It is observed that the distribution is quite homogeneous, with the vast majority of cells presenting a voltage in the range [0,65 V; 0,70 V]. This suggests that the design of the fuel cell and its hydrodynamics are highly suitable, facilitating consistent performance across all cells regardless of their position within the stack. Some discrepancy is nevertheless observed for the first cells probably due to potential unequal gas distribution or even to the lower temperatures they might present, but the difference between the highest and lowest voltages in the stack is at around 14% which is relatively acceptable. For comparison, at similar magnitudes of current, the 5 cell stack exhibited voltage discrepancies exceeding 30% despite its smaller size and lower number of cells, which might suggest that the design of the 5 cell experimental bench was not as optimal as it is observed at the Symbio fuel cell.

Overall, these findings underscore the effectiveness of the fuel cell's design and hydrodynamics, which contribute to a highly homogeneous voltage distribution across the cells in the stack. The minor discrepancies observed in the initial cells do not significantly impact the overall performance, as the voltage difference remains within an acceptable range.

- Water management

A series of experiments were conducted to investigate and describe in more detail the humidification process and the water management in the Symbio fuel cell. These experiments will be presented in the following sections.

(i) **Temperature gradient in the humidifier**

Firstly, the hypothesis tested aimed to ascertain whether the temperature gradient between both extremities of the membrane, which separates the dry chamber and the wet chamber of the humidifier, could be considered negligible. The temperature gradient is formed across the membrane when there is a difference in the temperature of each chamber. This gradient can have a notable influence on the humidifier's membrane and impact the efficiency and effectiveness of the humidification process.

If the temperature gradient is too high, it can potentially overwhelm the capacity of the humidifier to supply moisture. It can influence the durability and longevity of the humidifier's membrane, causing expansion and contraction of the membrane material, which may lead to

mechanical stress and potential damage over time, which means it is essential to consider the temperature gradient carefully.

The considerations will be based on the equation presented below, where the coefficient *k* represents the thermal conductivity, d_m represents the membrane thickness, A the membrane surface area and Cp the heat capacity of water. The temperatures T_s^w, T_s^d, T_{FC}, and T_{air}^{in} correspond respectively to the temperature of the membrane surface in the wet chamber, the temperature of the membrane surface in the dry chamber, the temperature in the fuel cell and the temperature of the inlet steam of air.

$$\frac{k}{d_m}(T_s{}^w - T_s{}^d) = \frac{\dot{n}_T^{out}.C_P(T_{FC} - T_{air}^{in})}{A} \tag{29}$$

The thermal conductivity *k* was assumed to be of 0,1 W/m.K.[7] Whereas the other factors had their values predefined based on thermodynamic properties and general norms, the thickness of the membrane was considered in the range [10,0 μm; 25,0 μm]. Those are values that can be found on the market from different fabricants, and the purpose was to test if the hypotheses would be confirmed for the upper range of values. The difference $T_s^w - T_s^d$ can give us an idea about the magnitude of the temperature gradient in the membrane and it is directly influenced by its thickness.

The difference $T_s^w - T_s^d$ for the low range of values (10,0 μm) was found to be of 0,25ºC, which is fairly negligible considering the magnitude of other temperatures involved. For the upper range of values, the difference between both surfaces was found at 0,63ºC, which is nonetheless still negligible for the scenario of the experiment. As a result, it can be concluded that the initial hypothesis holds true, and the temperature gradient across the membrane will be exceptionally small. This finding allows for better control of the tests and ensures improved durability for the membrane.

(ii) **Ratio of moist transferred in the humidifier**

The next step to better interpret the process of humidification is to estimate the ratio of moisture that is actually transferred from the wet chamber to the dry chamber. A scheme of the water transfer process inside the humidifier is shown below.

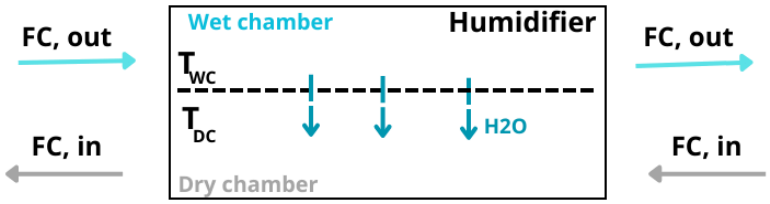

Figure 25: scheme of the water transfer in the humidifier

It is possible to observe that a fraction of water will be transferred through the membrane, whereas the moisture remaining in the wet stream will be later condensed. The purpose is then to estimate the ratio of the moist that is transferred rather than retained. In order to do so, two methods were considered: (i) an empirical one, with measures collected directly from the Symbio cell in one of the tests that were carried out and (ii) a theoretical one, based on a model using tabulated values.

For the first scenario, the water content produced at the 42,0 A test was considered, and the time span for this production was 16 minutes. The total amount of water produced could be calculated by the development of Faraday law as explained before. The amount of water retained was then collected at the condenser at the end of the time span, and the amount was then quantified using algebraic correlations based on the dimensions of the container (a cylinder of 70,0 mm diameter, and the water content filling this cylinder had a 37,0 mm height).

Considering the total amount of water produced in the test as $\dot{n}^{total}_{water,\,16}$ and the water retained as $\dot{n}^{retained}_{water,\,16}$, the ratio of water transferred to the dry chamber could be found by the relation $1 - \frac{\dot{n}^{retained}_{water,\,16}}{\dot{n}^{total}_{water,\,16}}$. The value for the experimental test was found to be 45,9%, which means that

during those 16 minutes in which the fuel cell was running at 42,0 A, about 46% of the moisture present in the outlet stream was transferred to the dry chamber.

The same procedure was applied for a theoretical test in order to check if the experimental data was coherent with the theory used to describe the water transfer phenomena. For this theoretical test, it was considered that the temperature of the air entering the humidifier was 20ºC with a dew temperature of 3ºC - that is, the stream had the same level of moisture of a saturated stream at 3ºC ($P_{partial}(air,\ inlet) = P_{sat}(3°C)$). The Buck equation (18) was once again used to calculate the partial pressure of water. Finally, the temperature of the stream leaving the fuel cell (corresponding to the wet stream entering the humidifier, T_{in}^{wet}) was assumed to be of 55ºC with a relative humidity of 95% ($RH_{FC,out} = 0,95$). These values were coherent with the ensemble of data collected during the tests and standard values found on bibliography for this type of process.

The current running through the fuel cell was also assumed to be at 42,0 A in order to avoid possible imprecisions due to different experimental conditions, although the intensity of current is not supposed to interfere directly in the ratio of water transferred to the dry chamber. The total amount of water produced was once again found using the Faraday law whereas the amount of water transferred between the membrane was calculated by the difference of moist content in the outlet and inlet streams of the dry chamber. The value was then found at 54,3%, slightly higher than for the first scenario.

Although there is a difference of about 10% between the results found for the two cases studied, it is clear that the values are in a close range, which validates the interpretation of the humidification process in the fuel cell. Overall, around half of the moisture produced was being transferred to the dry chamber. This result highlights the humidifier's efficiency in delivering moisture to the inlet stream and reinforces its effectiveness in promoting optimal conditions requiring controlled humidity levels. It is nonetheless important to highlight that further tests must be carried out in order to seek for better accuracy, since these are among the first tests to be conducted.

9. Discussion

Throughout the course of the project on the 5 cell stack fuel cell and the Symbio fuel cell, several important points have been identified. This section aims to summarize the key findings, focusing on the effectiveness of the system, potential problems that may arise during scale-up for market exploitation, and potential solutions to overcome those challenges.

The project has demonstrated the overall effectiveness of the PEMFC system. Extensive testing and analysis have shown that the Symbio system efficiently converts chemical energy into electrical energy, producing clean power with low emissions. The tests on the 5 cell stack experimental bench were slightly less successful overall, showing higher levels of instability and higher voltage gaps between each cell. This shows the importance of an adequate design and good control of hydrodynamics for an optimal operation, which was successfully obtained on the platform.

The experimental observations also revealed that the performance of both cells improved with longer operating periods compared to when they were freshly turned on. The cells exhibited greater stability, and water management was notably improved. This is not necessarily the case if exploited for much longer periods since the aging of the equipment, the membrane and the catalyst can become an issue for the optimal operation. This concern is not unique to PEMFC mobility but applies to aging challenges faced by both fossil fuel-based and conventional electrical mobility solutions. Nevertheless, the study verified that PEMFCs can exhibit great durability when operated under appropriate conditions.

For the stoichiometric of reactants, it was also demonstrated that the system showed better results for higher stoichiometric factors in both hydrogen and air streams. For the Symbio fuel cell, the tests carried out at $\lambda_{air} = 3{,}0$ rather than $\lambda_{air} = 2{,}5$ could generate around 4% more power, besides better heat control and water management at these conditions. Higher hydrogen stoichiometric factors could also lead to an increase in the performance of the fuel cell and promote more stability, besides avoiding an eventual suffocating of the system.

Another key aspect to be discussed is the water management in the fuel cells. Overall, the management of water within the fuel cell system was highly efficient and well-regulated. The

appropriate balance of water content was maintained, ensuring optimal functioning and preventing any detrimental effects for both the 5 cell stack experimental bench and the Symbio fuel cell. For the former, the control mechanisms in place effectively controlled the water levels, preventing excessive accumulation or depletion. For the Symbio fuel cell on the other hand there were a few issues with water control at some point, and excessive water accumulation was observed. The issue was solved by elevating the fuel cell to an angle and position that would facilitate the evacuation of water, which reinforces the importance of an architecture that favors optimal hydrodynamics for a fuel cell system.

Finally, it is important to discuss the efficiency and performance of the Symbio system. From the results presented in the previous sections and the Figure18, it can be deduced that the efficiency of the Symbio fuel cell was at around $\eta_{symbio\ FC} = 51\%$. This value is coherent with bibliographic values, as hydrogen fuel cells can usually achieve electrical efficiencies ranging from 40% to 60%.[13] This is well above the average for traditional combustion-based power generation methods. For the performance, the Symbio fuel cell went up to 2,5 kW due to the load receptor limitation, but could otherwise go even further on with adequate equipment and the right operation conditions as it has a capacity of 5,0 kW.

10. Conclusion

The performance results have met the initial expectations, indicating the potential for the technology to contribute significantly to sustainable energy solutions. As expected, the high power density and rapid response time of the PEMFC make it an attractive choice for urban and peri-urban mobility. Further tests must nevertheless be carried out in the platform, specially for the higher values of current, which could unfortunately not be reached during a large period of the project due to the flowmeter limitations. It would be interesting to eventually test the Symbio fuel cell in its whole capacity by using a higher capacity load.

It is equally valid to do more experiments in pressures exceeding 1,0 bar, since operating at elevated pressures can lead to increased power density and facilitates greater reactant delivery to the electrode surfaces, promoting therefore more efficient electrochemical reactions and enabling higher power output for a given cell size. More work could also be done in the

humidifier in order to optimize the moisture transfer thus improving the effectiveness of the proton exchange in the fuel cell.

Another concern might be the scaling up of the PEM fuel cell technology for widespread market exploitation. One significant issue that was not necessarily treated on the course of this project but definitely needs more research upon is the cost associated with materials and manufacturing processes. As the production volume increases, it becomes crucial to optimize material usage and streamline manufacturing techniques to achieve economies of scale. Additionally, the availability and affordability of key catalyst materials, such as platinum, may pose constraints when producing large quantities of fuel cells.

It's verified that the cost of material today is already lower than when the studies on PEMFC first began as several research has already been conducted on the matter. It remains crucial that these studies keep being carried out to make the technology more cost-friendly over time and then allow greater accessibility to the public. Continuous improvement in manufacturing processes and automation can contribute to cost reduction, as well as optimizing the assembly techniques, minimizing material waste, and implementing quality control measures. Collaboration within the industry to establish standardized manufacturing protocols and sharing best practices can accelerate progress in this regard.

In order to overcome the challenges associated with scaling up the PEM fuel cell technology, it is also of great importance to address the durability and reliability with further research. While the current PEMFC technology has shown relatively satisfactory results compared to traditional mobility means, there is still room for improvement, and developing more robust and resilient PEMs, improving electrode architectures, and implementing effective contamination mitigation strategies are therefore vital steps. Close cooperation between academia, industry, and government entities is crucial to facilitate research and knowledge exchange, ultimately leading to enhanced durability and longevity of the fuel cell systems.[14]

The project has successfully demonstrated the effectiveness of the PEM fuel cell system, showing its potential as a clean energy solution. However, challenges remain when scaling up for market exploitation. Addressing cost factors, improving durability, and refining manufacturing processes are key areas of focus for future development. By investing in

research, innovation, and collaboration, the industry can overcome these challenges and unlock the full potential of PEM fuel cell technology for a sustainable energy future.

In conclusion, the realization of this project provided a comprehensive and insightful analysis of the promising technology of PEMFCs and its potential to assume an important role in the mobility industry. The report delved into various aspects of PEMFCs, including their working principles, materials, design considerations, and performance optimization techniques. Key challenges such as water management, durability, and system efficiency were investigated offering valuable insights and strategies. Experimental techniques and data analysis methods were employed to better understand the fundamental principles underlying PEMFCs in it. This project carried out over the last months will hopefully pave the way for advancements in this promising technology and collaborate for further future research and development efforts.

11. Appendix

Process Flow Diagram of the 5 cell stack

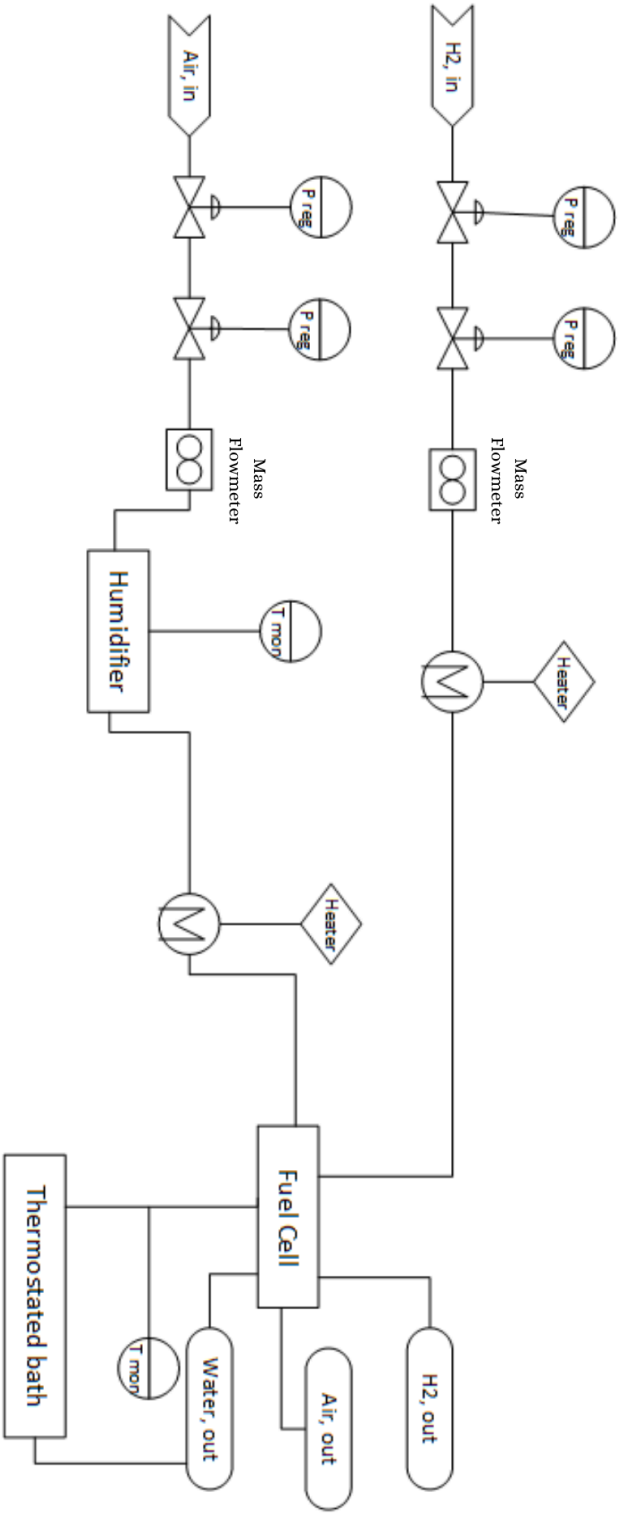

Process Flow Diagram of the Symbio 70 cell stack

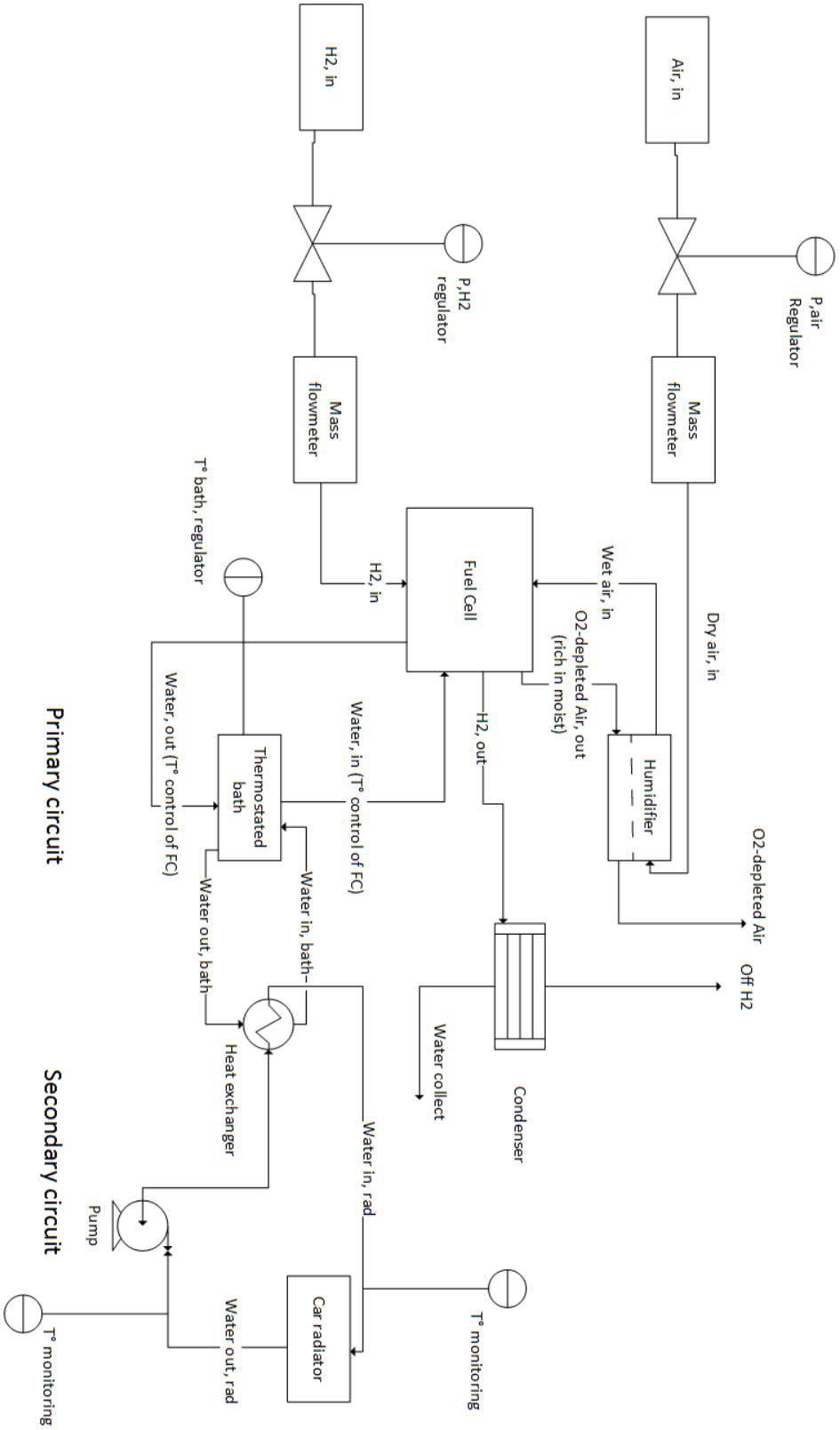

12. References

(1) Jeulin-Lagarrigue, Michaël. “Les COP : une brève histoire de la COP1 à la COP27 | Compte CO2”. Compte CO2 - La Carte CO2, un outil de lutte pour la préservation du climat, https://compteco2.com/article/historique-cop-conference-des-parties.

(2) Nations, United. “COP26: Together for Our Planet”. United Nations, https://www.un.org/en/climatechange/cop26.

(3) What Is the Impact of Transport on Climate Change? https://www.activesustainability.com/sustainable-life/impact-transport-climate-change/.

(5) Reversible Cell Potential - an overview | ScienceDirect Topics. https://www.sciencedirect.com/topics/engineering/reversible-cell-potential.

(6) Auer E, Freund A, Pietsch J, Tacke T. 1998. Carbons as supports for industrial precious metal catalysts. Applied Catalysis A: General. 173(2):259-271.

(7) Dicks, Andrew, e D. A. J. Rand. Fuel cell systems explained. Third edition, Wiley, 2018.

(8) Bridgeman and Aldrich, 1964, Bridgeman, O.C.; Aldrich, E.W., Vapor Pressure Tables for Water, J. Heat Transfer, 1964, 86, 2, 279-286

(9) Ibrahim Dincer, Calin Zamfirescu (2014). "4.4.7 Direct Methanol Fuel Cells". Advanced Power Generation Systems. doi:10.1016/B978-0-12-383860-5.00004-3

(10) SHIRSATH, Anatrao Vijay (2021) “Experimental development of the electrochemical pressure impedance spectroscopy for characterization of transport phenomena in membrane fuel cell”.

(11) Hou, Xukai, et al. “A Hybrid Combined Heat and Power System Based on PEM Fuel Cell Design for High-Speed Zero Carbon Service Area”. International Journal of Hydrogen Energy, ScienceDirect.

(12) “Record 45 New Hydrogen Filling Stations Open in Europe in 2022 - Ryze Hydrogen”. Hydrogen Central, 9 de fevereiro de 2023, https://hydrogen-central.com/record-45-new-hydrogen-filling-stations-open-in-europe-2022-ryze-hydrogen/.

(13) Du Plooy, D., et al. “Adaptive purging control of hydrogen fuel cells for high efficiency applications”. 2018 International Conference on the Domestic Use of Energy (DUE), IEEE, 2018, p. 1–6. DOI.org (Crossref), https://doi.org/10.23919/DUE.2018.8384402.

(14) Lotrič, Andrej, et al. “Life-Cycle Assessment of Hydrogen Technologies with the Focus on EU Critical Raw Materials and End-of-Life Strategies”. International Journal of Hydrogen Energy, vol. 46, on 16, march of 2021, p. 10143–60. DOI.org (Crossref), https://doi.org/10.1016/j.ijhydene.2020.06.190.

(15) Holton, Oliver T., e Joseph W. Stevenson. “The Role of Platinum in Proton Exchange Membrane Fuel Cells”. Platinum Metals Review, vol. 57, on 4, october 2013, p. 259–71. DOI.org (Crossref), https://doi.org/10.1595/147106713X671222.